Collins–Soper Kernel from Lattice QCD: towards physical-continuum limit

Xiang Gao

LaMET 2026, Jagiellonian University, Cracow, Poland, Jul 6 – 9, 2026

Transverse-momentum-dependent distributions

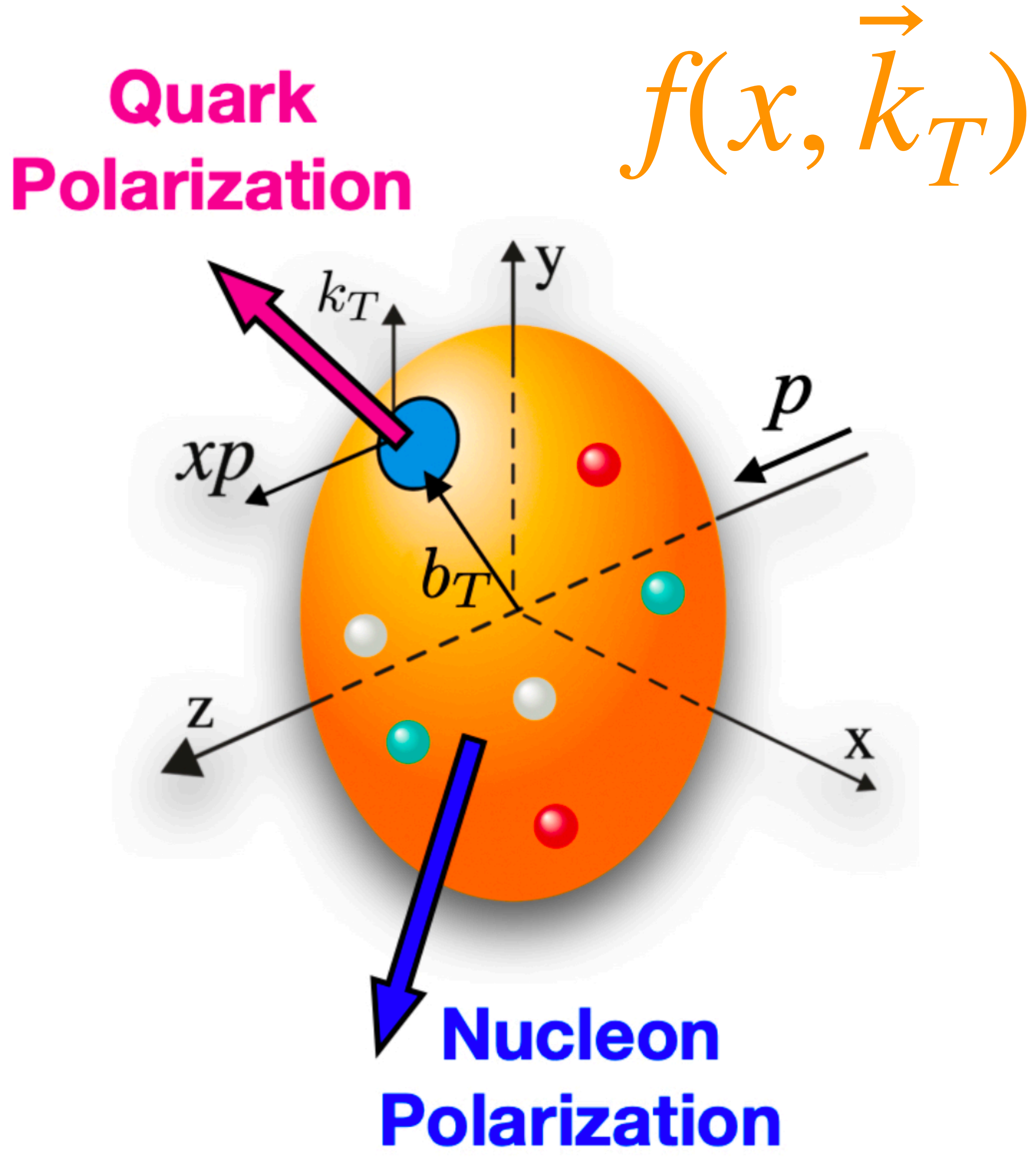

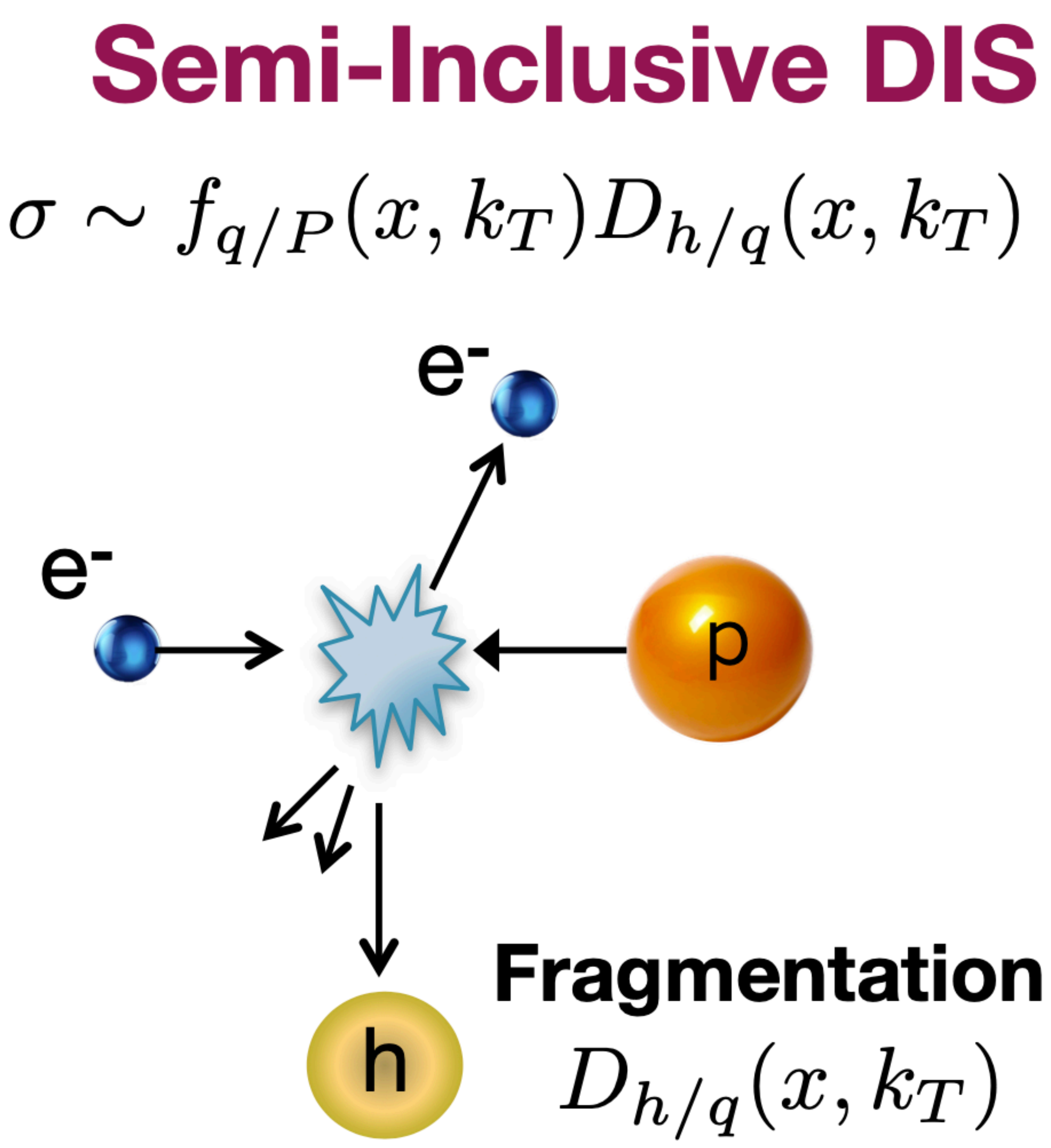

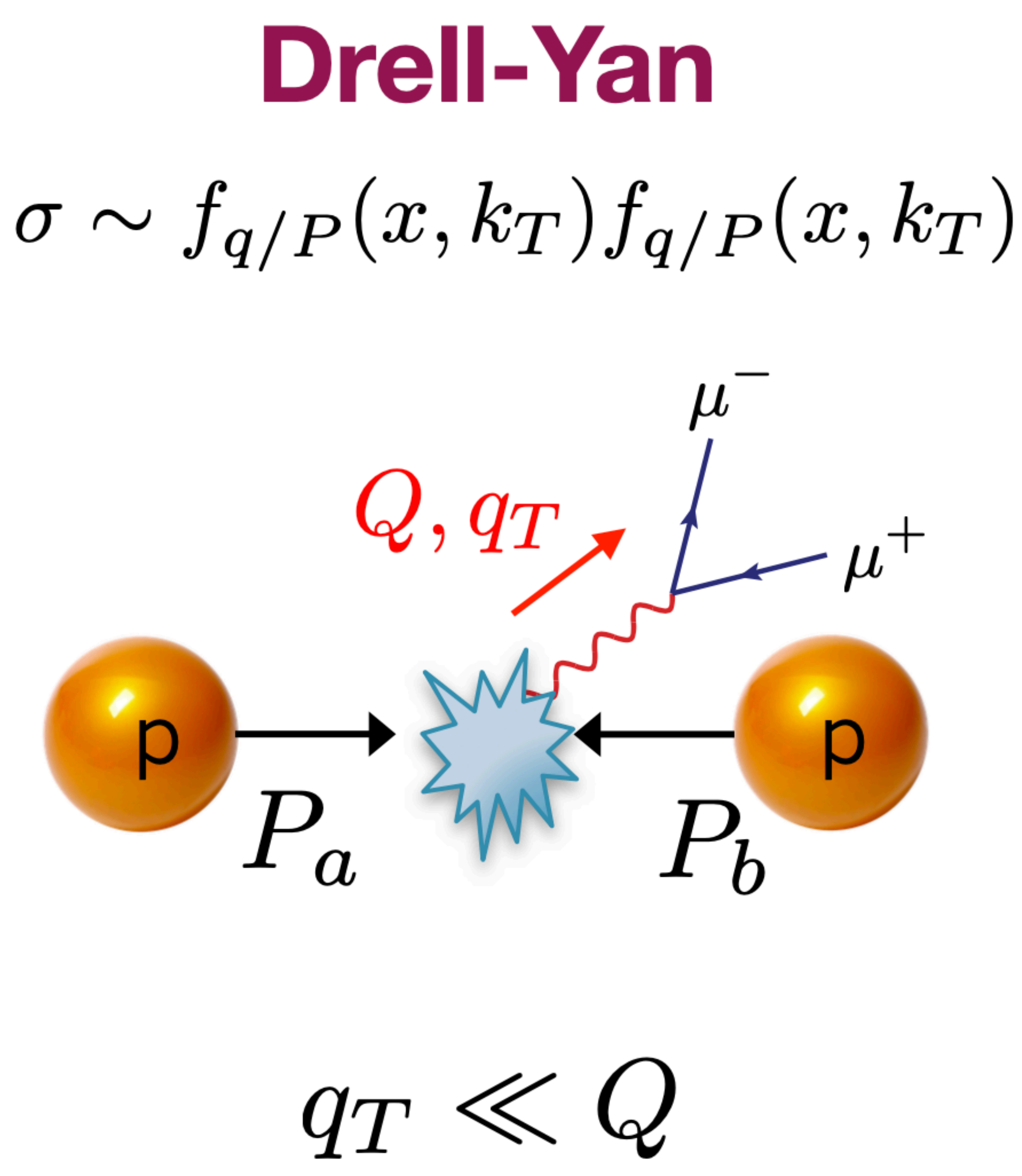

- 3D image: longitudinal momentum fraction x and confined motion $\vec{k}_T$.
- Essential for spin-orbit structure and precision QCD phenomenology.

Nonperturbative TMDs remains underconstrained

- Helicity and unpolarized TMD ratio

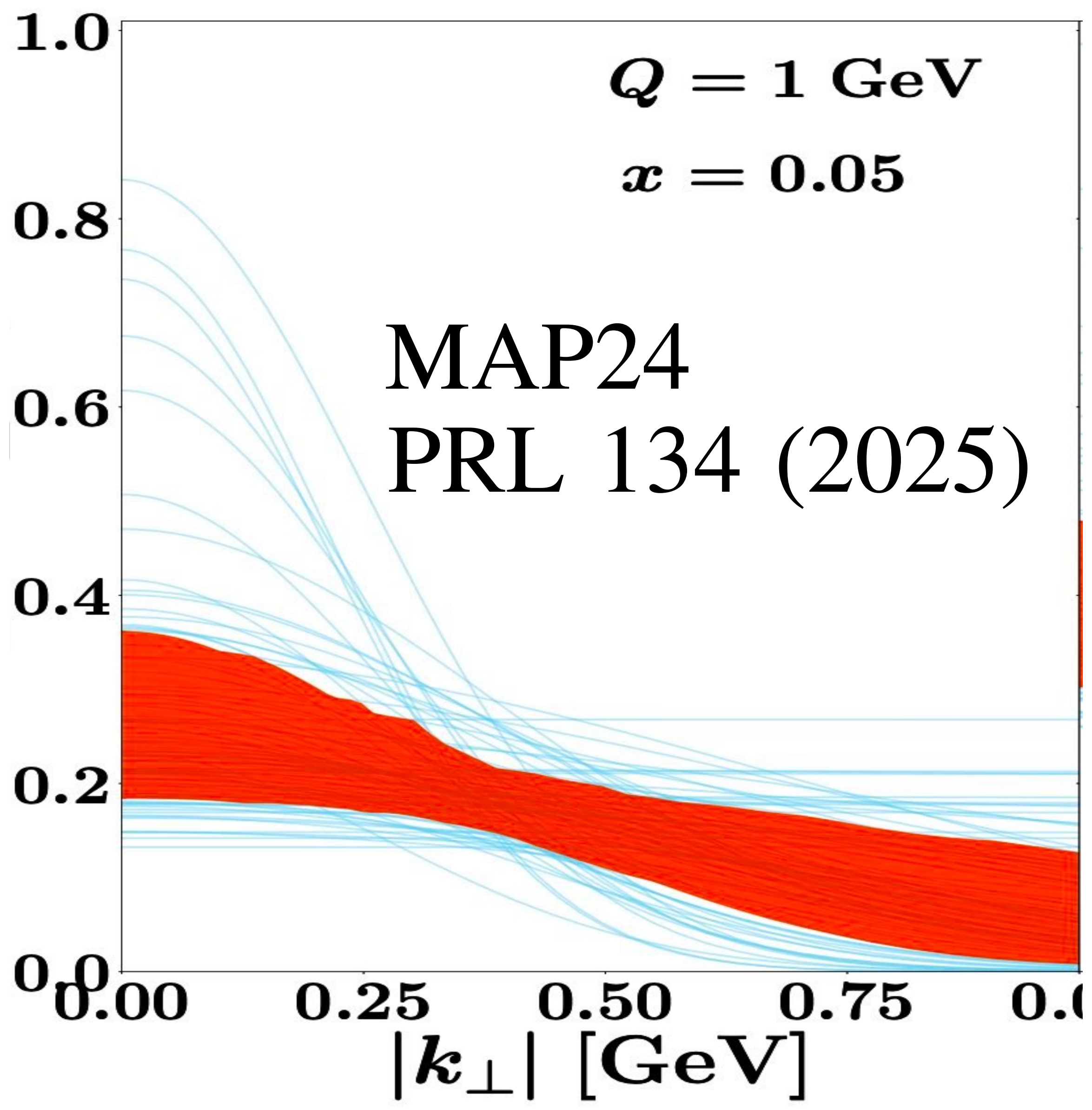

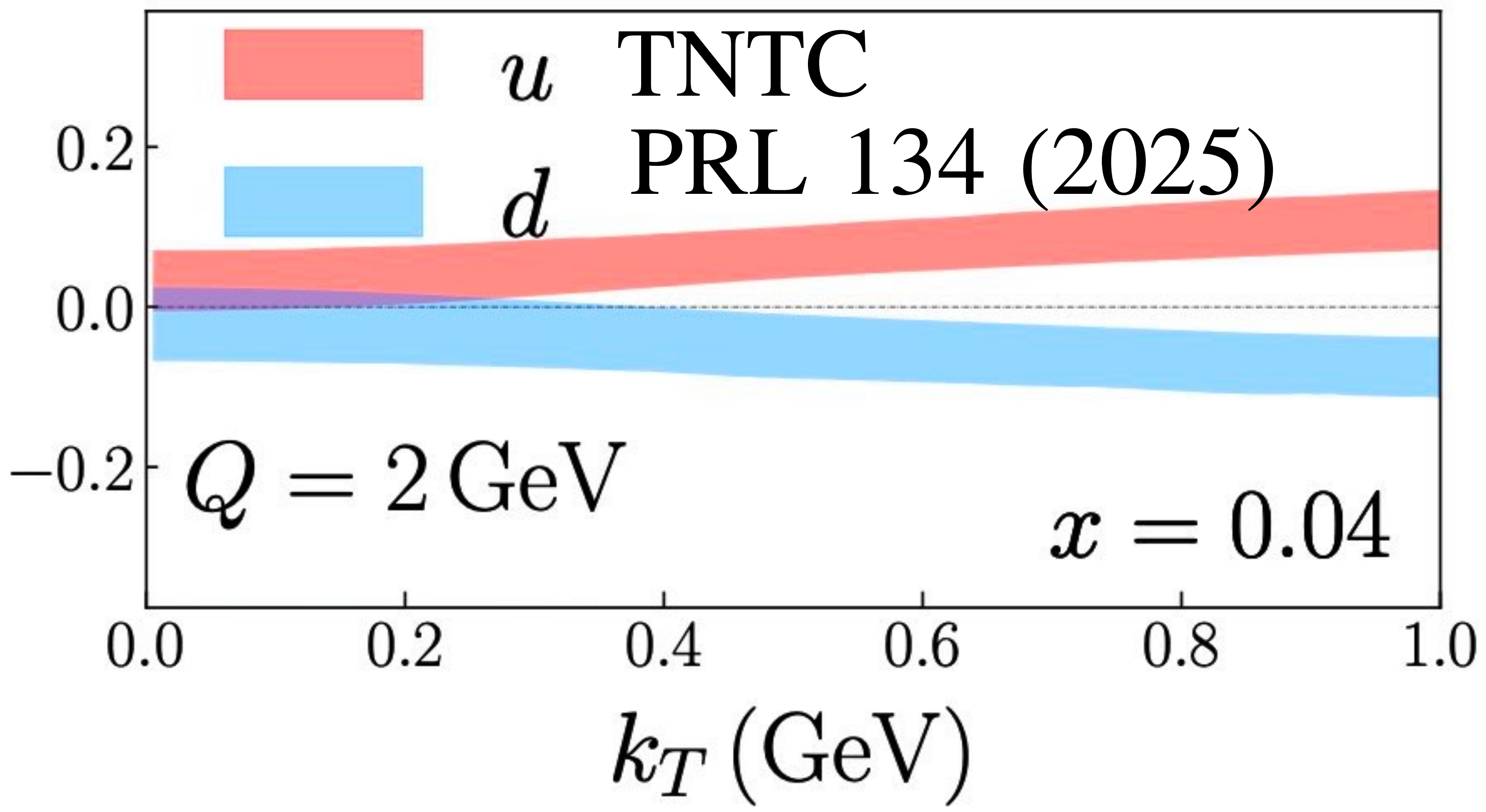

- Collins-Soper (rapidity evolution) kernel

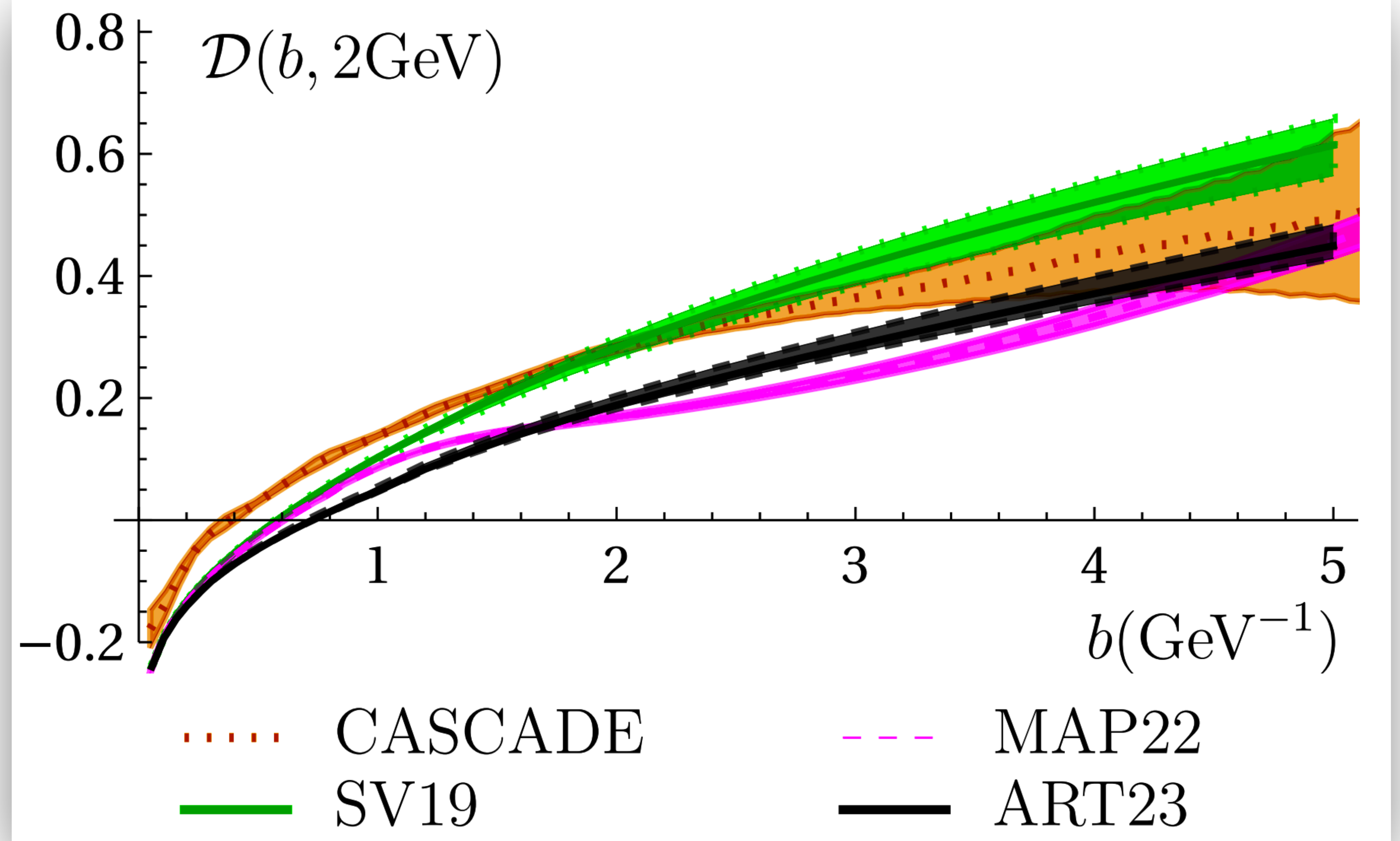

- Sparse data leave sizable freedom in the nonperturbative region.
- Different parametrizations can give visibly different TMD physics.
- Lattice QCD provides complementary first-principles constraints.

TMDs from lattice: quasi-TMDs

- Ji, Liu and Liu, NPB 955 (2020), PLB 811 (2020);
- A. Vladimirov, A. Schäfer Phys.Rev.D 101 (2020), 074517
- I. Stewart, Y. Zhao et al., JHEP 09 (2020) 099
- X. Ji et al., Phys.Rev.D 103 (2021) 7, 074005
- I. Stewart, Y. Zhao et al., JHEP 08 (2022) 084

- Equal-time GI correlators with spacial separations.
- Approaching light-cone TMDs in the large momentum limit (LaMET).

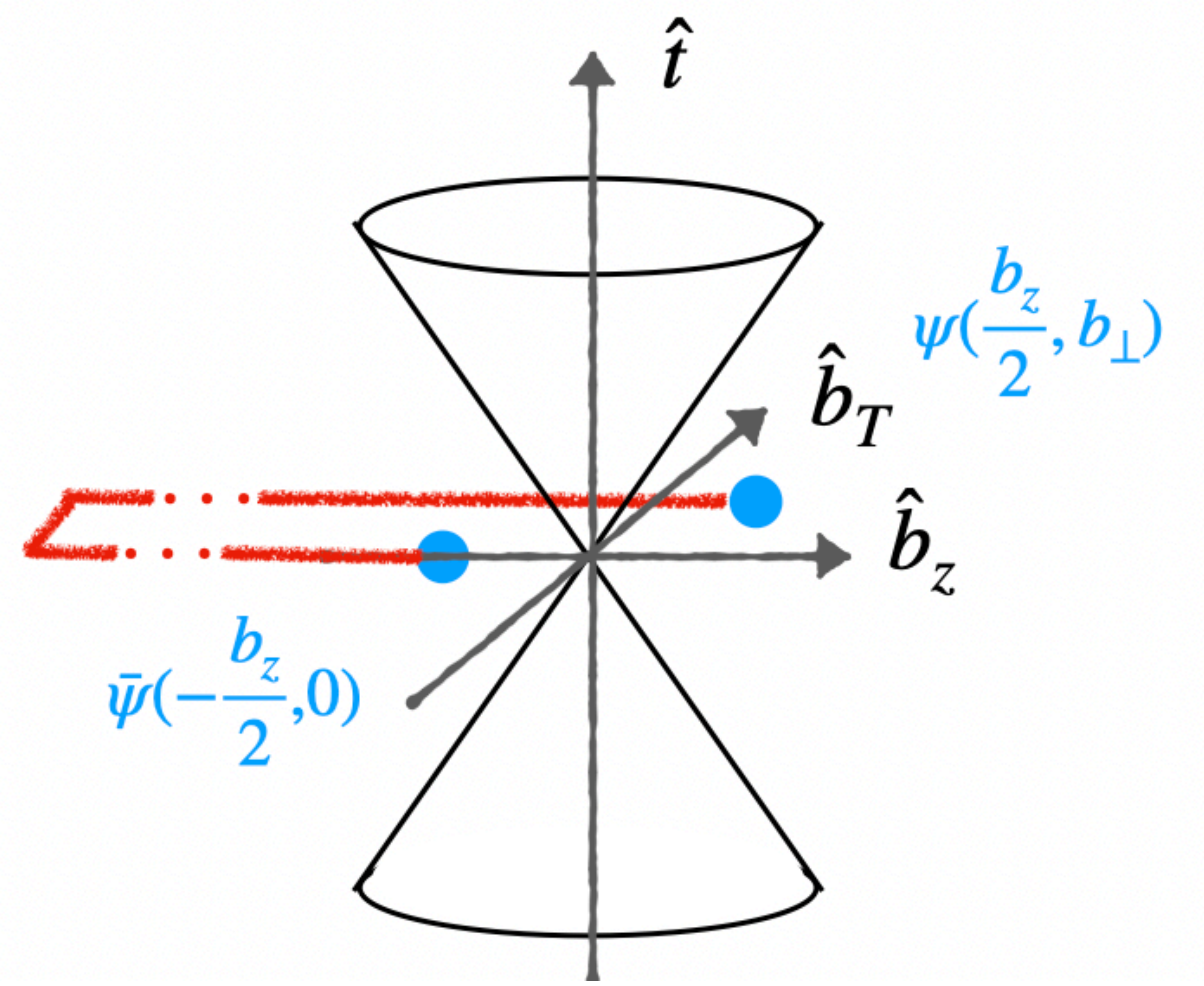

$P_z \to \infty$

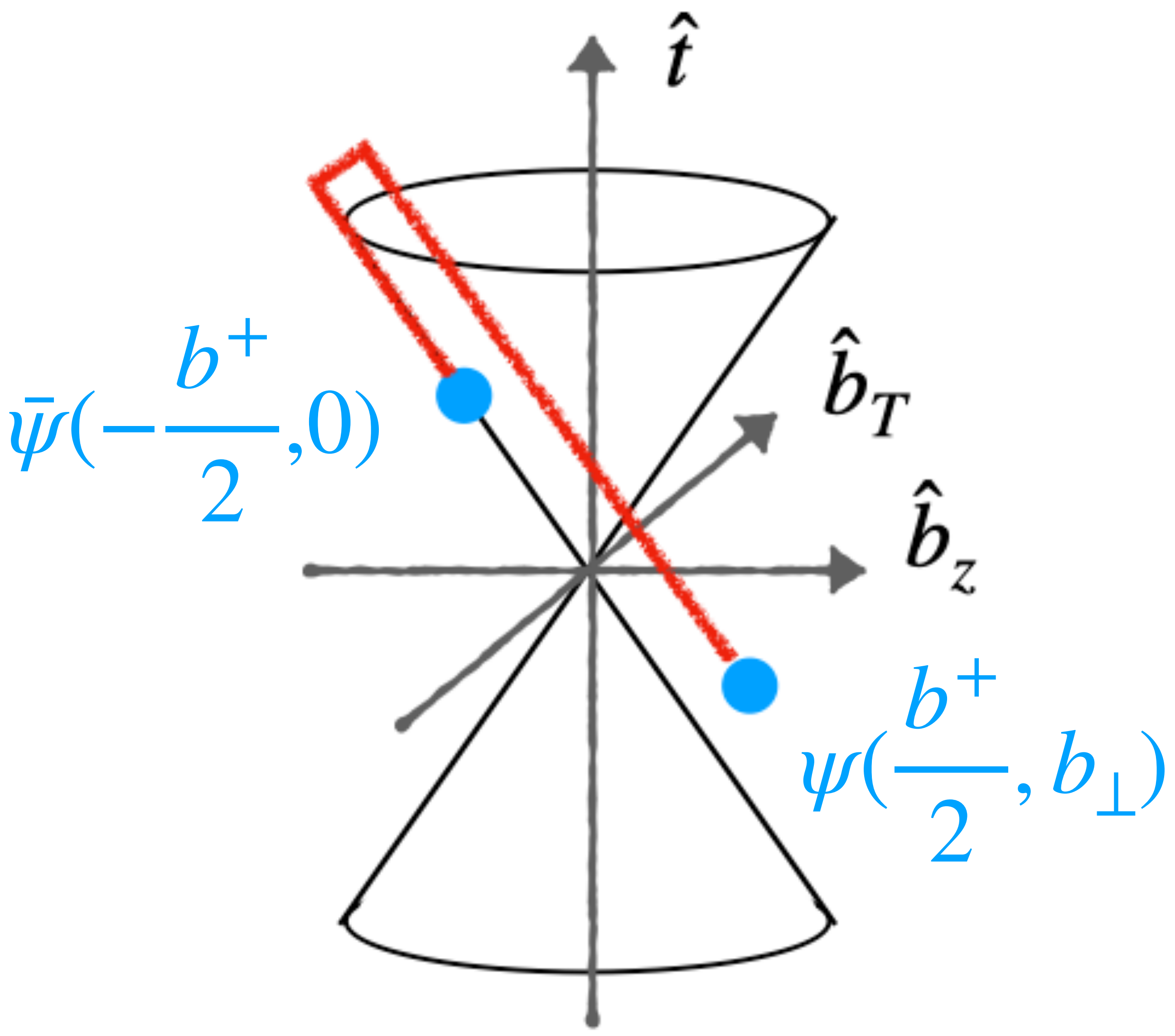

Quasi TMD

$$\langle P|\overline{\psi}(\frac{b^z}{2}, b_\perp)\Gamma W_{\sqsupset^z}\psi(-\frac{b^z}{2}, 0)|P\rangle$$
$$= \langle P|\overline{\psi}(\frac{b^z}{2}, b_\perp)\Gamma \psi(-\frac{b^z}{2}, 0)|_{A^z=0}|P\rangle$$

Light-cone TMD

$$\langle P|\overline{\psi}(\frac{b^+}{2}, b_\perp)\Gamma W_{\sqsupset^+}\psi(-\frac{b^+}{2}, 0)|P\rangle$$
$$= \langle P|\overline{\psi}(\frac{b^+}{2}, b_\perp)\Gamma \psi(-\frac{b^+}{2}, 0)|_{A^+=0}|P\rangle$$

The universality class of quasi-distributions

- Physical gauges, including Coulomb gauge (CG) and axial gauge, define quasi-PDF/TMD operators without Wilson lines.
- In the large-momentum limit, they approach the same light-cone TMD.

- **XG**, W.-Y. Liu, Y. Zhao, PRD 109 (2024) 9, 094506
- Y. Zhao, PRL 133 (2024) 24, 241904

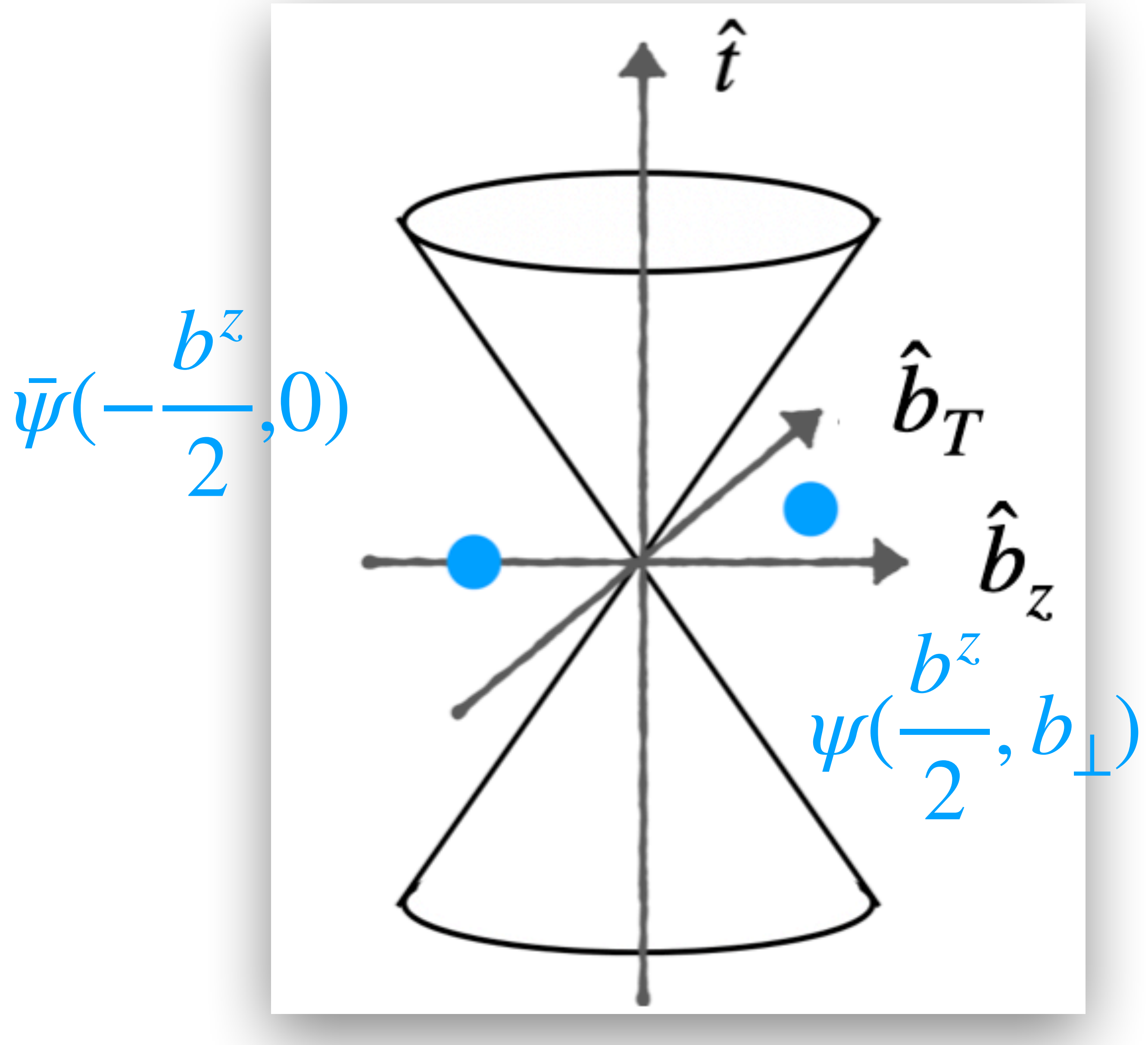

Quasi TMD

$$\langle P|\overline{\psi}(\frac{b_z}{2},b_\perp)\Gamma\psi(-\frac{b_z}{2},0)\,|_{\vec{\nabla}\cdot\vec{A}=0}\,|P\rangle$$
$$|_{A^z=0}$$
$$|_{A^t=0}\ \cdots$$

$P_z \to \infty$

Physical gauge
$\to A^+$ gauge

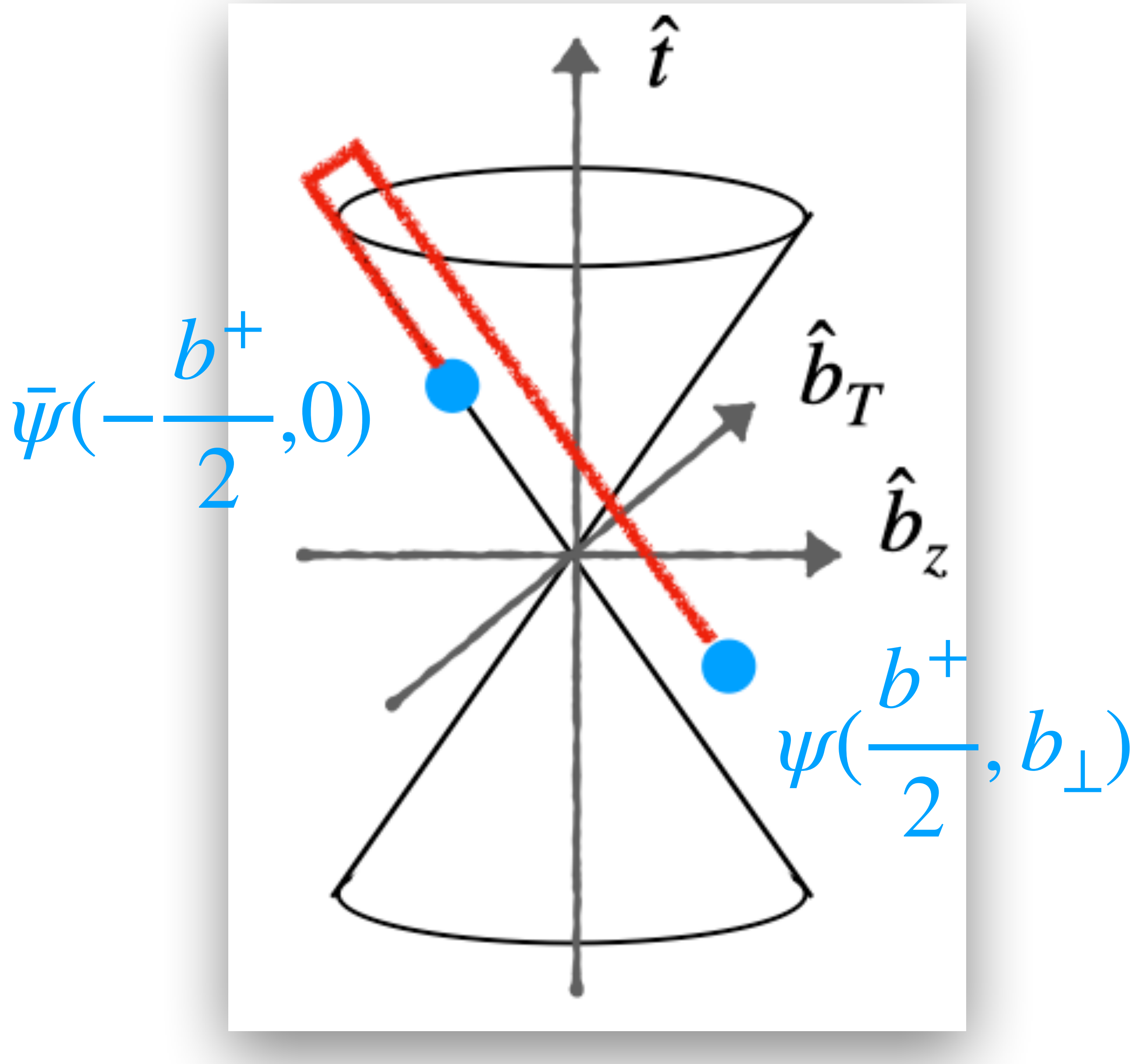

Light-cone TMD

$$\langle P|\overline{\psi}(\frac{b^+}{2},b_\perp)\Gamma W_{\sqsupset^+}\psi(-\frac{b^+}{2},0)|P\rangle$$
$$=\langle P|\overline{\psi}(\frac{b^+}{2},b_\perp)\Gamma\psi(-\frac{b^+}{2},0)\,|_{A^+=0}\,|P\rangle$$

Large P_z expansion and perturbative matching

- Ji, Liu and Liu, NPB 955 (2020), PLB 811 (2020);
- A. Vladimirov, A. Schäfer Phys.Rev.D 101 (2020), 074517
- I. Stewart, Y. Zhao et al., JHEP 09 (2020) 099
- X. Ji et al., Phys.Rev.D 103 (2021) 7, 074005
- I. Stewart, Y. Zhao et al., JHEP 08 (2022) 084
- Y. Zhao, PRL 133 (2024) 24, 241904

Quasi TMD beam function

Collins-Soper kernel

$$\sqrt{S_I(\vec{b}_T,\mu)}\tilde{f}(x,\vec{b}_T,\mu,P_z) = H_f(\mu,xP_z)e^{\frac{1}{2}\gamma_\zeta(\mu,b_T)\ln\frac{(2xP_z)^2}{\zeta}}f(x,\vec{b}_T,\mu,\zeta)\{1+\mathcal{O}[\frac{1}{(xP_zb_T)^2},\frac{\Lambda_{\rm QCD}^2}{(xP_z)^2}]\}$$

Soft-factor

Physical TMD

$$P_z \lesssim a^{-1}$$

- **Large momentum expansion (LaMET)** towards light-cone TMDs.
- **Perturbative matching** $H_f(\mu, xP_z)$ and **power corrections** are scheme dependent: GI/CG/other physical gauge.

Collins-Soper kernel from CG quasi-TMD

perturbative correction

$$\gamma^{\overline{\mathrm{MS}}}(b_\perp,\mu) = \frac{1}{\ln(P_2/P_1)} \ln\left[\frac{\tilde{\phi}(x,b_\perp,P_2,\mu)}{\tilde{\phi}(x,b_\perp,P_1,\mu)}\right] + \delta\gamma^{\overline{\mathrm{MS}}}(x,\mu,P_1,P_2)$$

$P_1 \to P_2$ quasi-TMDWF

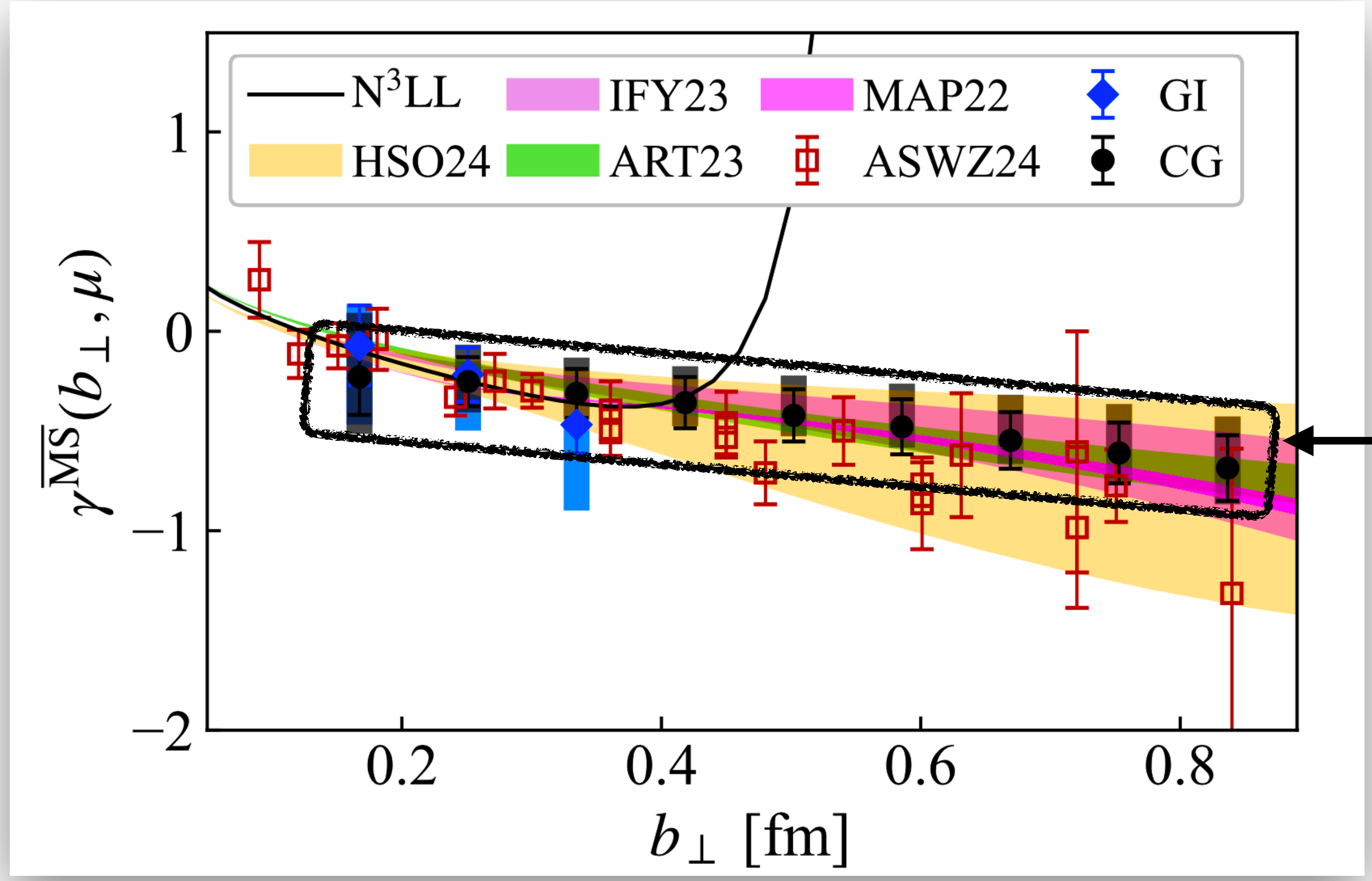

- Consistent with most recent global fits and GI quasi-TMD approach with improved signal in nonperturbative $b_\perp$ region.

• D. Bollweg, **XG**, S. Mukherjee, Y. Zhao, PLB 852 (2024) 138617

Ratios of TMDPDFs from quasi-TMD beam functions

Quasi TMD beam function

Physical TMD

$$\sqrt{S_I(\vec{b}_T,\mu)}\,\tilde{f}(x,\vec{b}_T,\mu,P_z) = H_f(\mu,xP_z)e^{\frac{1}{2}\gamma_\zeta(\mu,b_T)\ln\frac{(2xP_z)^2}{\zeta}} f(x,\vec{b}_T,\mu,\zeta)\{1+\mathcal{O}[\frac{1}{(xP_zb_T)^2},\frac{\Lambda_{\rm QCD}^2}{(xP_z)^2}]\}$$

$$\frac{\tilde{f}_1(x,b_T,P_z,\mu)}{\tilde{f}_2(x,b_T,P_z,\mu)} = \frac{f_1(x,b_T,\zeta,\mu)}{f_2(x,b_T,\zeta,\mu)} + \mathrm{p.c.}$$

- Ratios cancel soft factor & perturbative corrections & scale evolution.
- **Renormalization-group-invariant** (RGI).
- **Valid to all orders** in perturbation theory up to power corrections.

Lattice benchmark for $u-d$ heli. and unpol. TMDPDFs

$$\frac{g_{1L}^{\Delta u^+-\Delta d^+}(x,b_T)}{f_1^{u_v-d_v}(x,b_T)}\frac{1}{g_A}=\frac{\tilde{g}_{1L}^{\Delta u^+-\Delta d^+}(x,b_T)}{\tilde{f}_1^{u_v-d_v}(x,b_T)}\frac{1}{g_A}$$

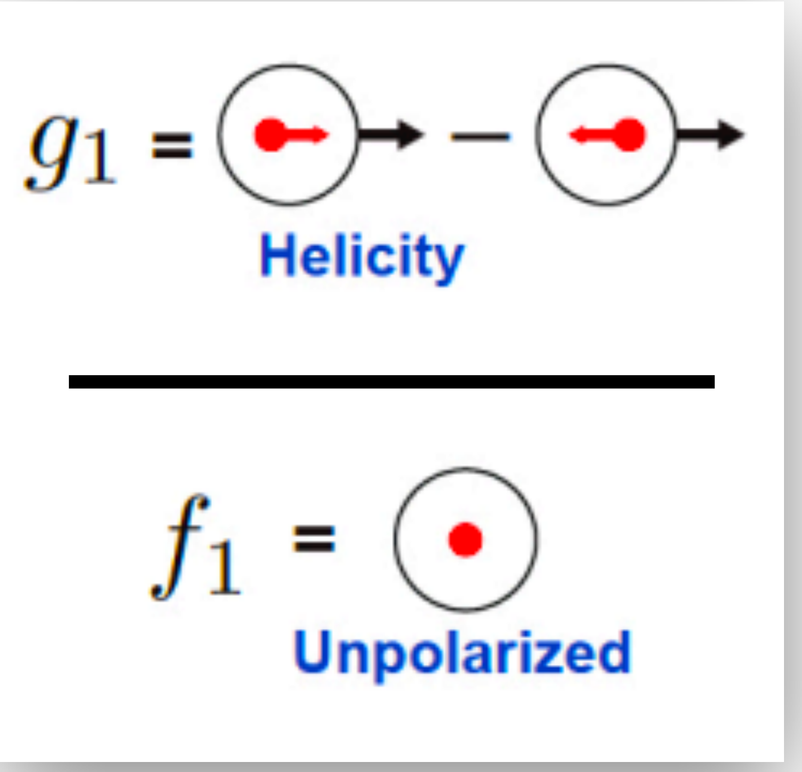

Lattice benchmark

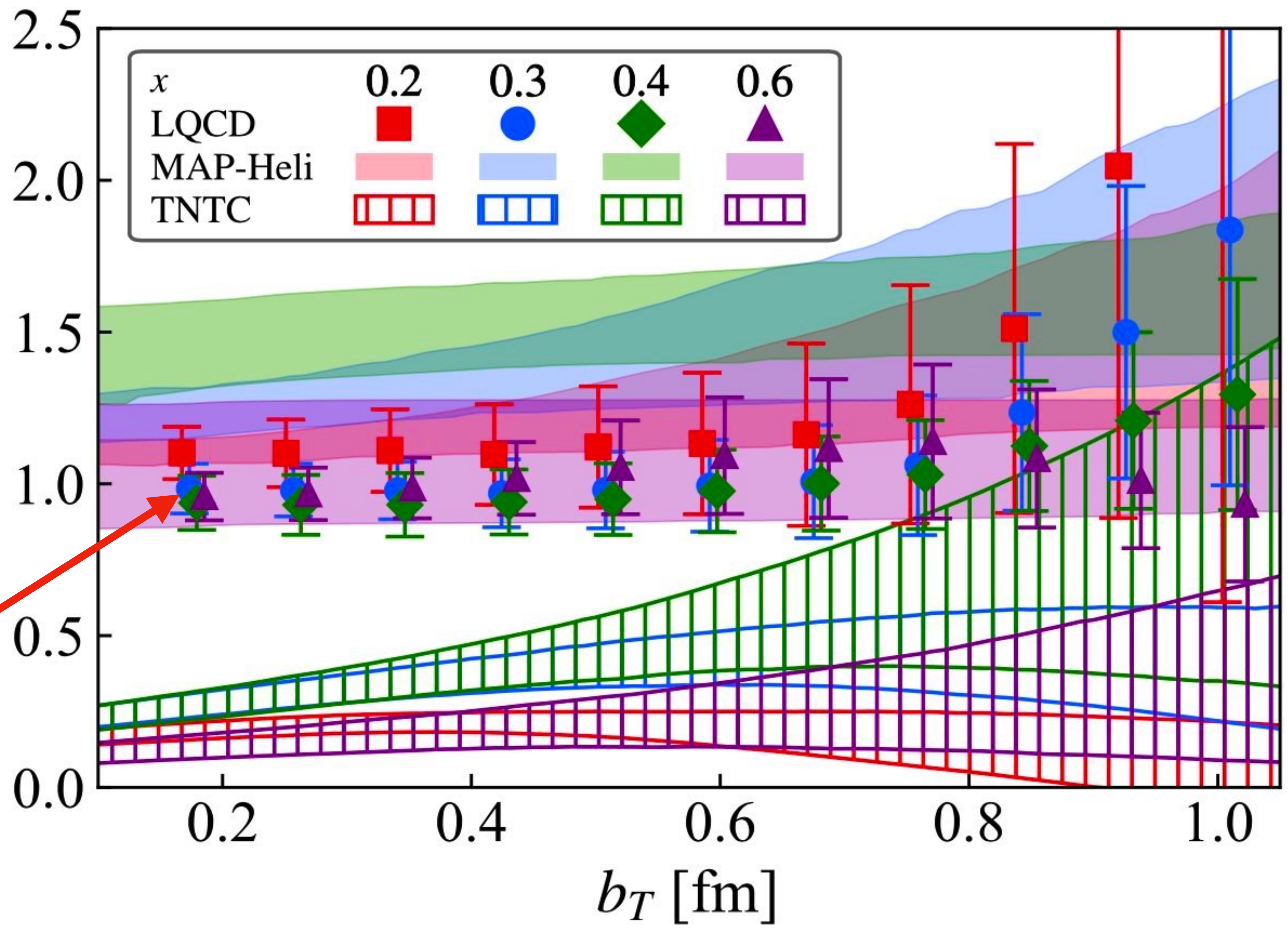

- D. Bollweg, **XG**, S. Mukherjee, Y. Zhao, PRL 135 (2025), 201901

- No strong dependence on b_T: longitudinal **spin polarization has limited impact** on the intrinsic transverse motion of quark inside nucleon.

Combining with soft function gives individual TMDPDFs: see Jinchen's talk today

Towards physical-continuum limit: CS kernel

- The CG quasi-distribution approach has shown great efficiency in computing nonperturbative TMDs.
- Next step: toward the physical-continuum limit, large momentum limit, …

Ongoing project: nonperturbative CS kernel $\gamma^{\overline{\rm MS}}(b_\perp, \mu)$ from quasi-TMD wave function

Clover valence quark on HISQ ensemble

a (fm)	N_s	N_t	m_π (MeV)	Volume L^3 (fm^3)	P_z (GeV)
0.040	64	64	136	$(2.56)^3$	0.00, 1.45, 1.94, 2.42
0.050	64	64	140	$(3.20)^3$	0.00, 1.16, 1.55, 1.94
0.050	80	80	140	$(4.00)^3$	0.00, 1.55, 1.86, 2.17
0.060	48	64	140	$(2.88)^3$	0.00, 1.29, 1.72, 2.15
0.060	64	64	135	$(3.84)^3$	0.00, 1.29, 1.61, 1.94
0.076	64	64	140	$(4.86)^3$	0.00, 1.27, 1.53, 1.78, 2.04

All at the physical point

Main systematics to control

- continuum extrapolation ($a^{-1} \to \infty$)
- power corrections ($P_z \to \infty$ extrapolation)
- finite volume effect

Towards physical-continuum limit: CS kernel

- The CG quasi-distribution approach has shown great efficiency in computing nonperturbative TMDs.
- Next step: toward the physical-continuum limit, large momentum limit, …

Ongoing project: nonperturbative CS kernel $\gamma^{\overline{\mathrm{MS}}}(b_\perp, \mu)$ from quasi-TMD wave function

Clover valence quark on HISQ ensemble

a (fm)	N_s	N_t	m_π (MeV)	Volume L^3 (fm^3)	P_z (GeV)
0.040	64	64	136	$(2.56)^3$	0.00, 1.45, 1.94, 2.42
0.050	64	64	140	$(3.20)^3$	0.00, 1.16, 1.55, 1.94
0.050	80	80	140	$(4.00)^3$	0.00, 1.55, 1.86, 2.17
0.060	48	64	140	$(2.88)^3$	0.00, 1.29, 1.72, 2.15
0.060	64	64	135	$(3.84)^3$	0.00, 1.29, 1.61, 1.94
0.076	64	64	140	$(4.86)^3$	0.00, 1.27, 1.53, 1.78, 2.04

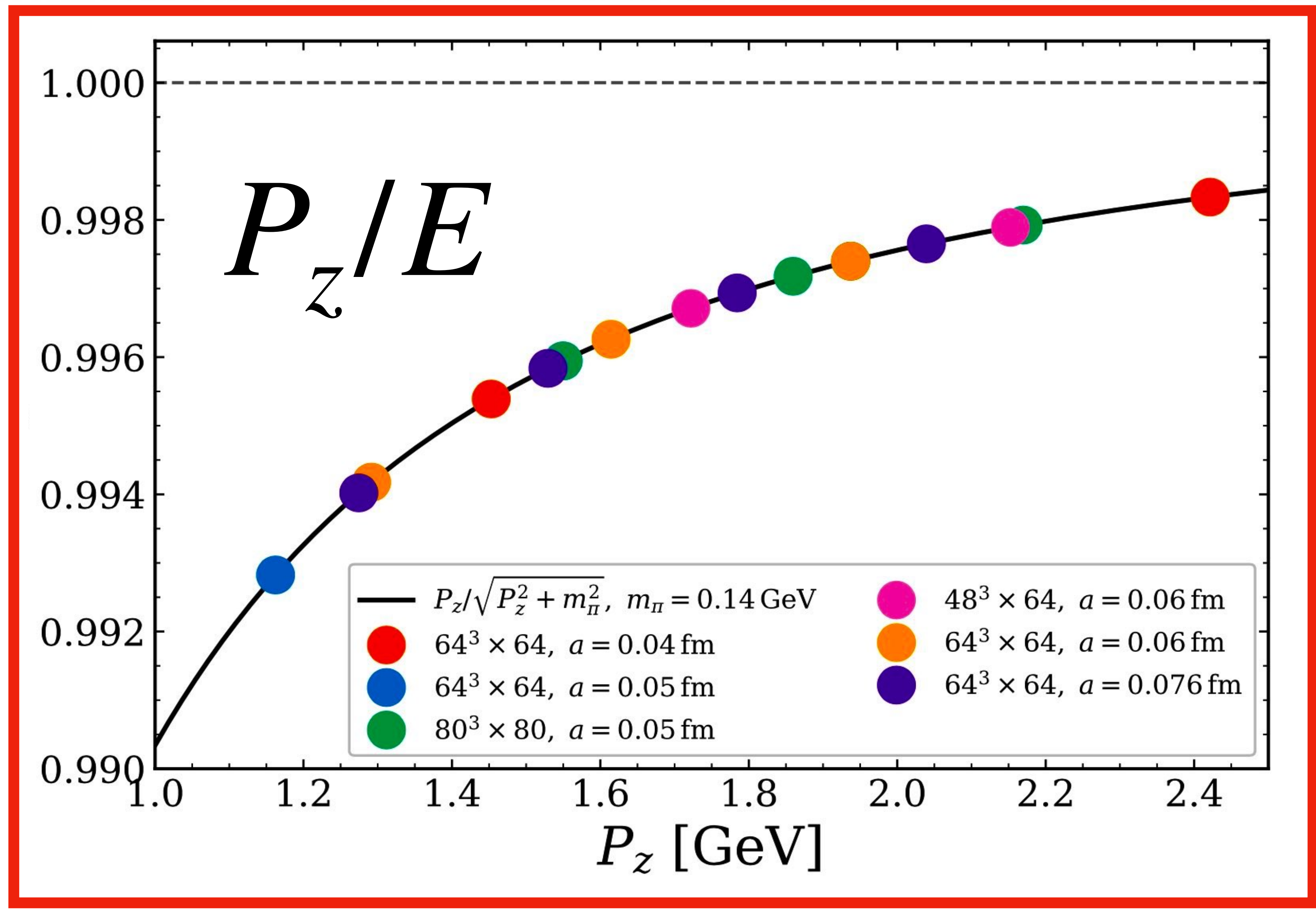

Large momenta boost: relativistic pion

$P_z/E \in [0.992, 0.999]$

Quasi-TMDWF matrix elements: local-case check

Bare matrix element at $b_T = b_z = 0$

$$\langle \Omega | \bar{\psi}(0,0)\Gamma\psi(0,0) | \pi^+, P_z \rangle = P_z \tilde{\phi}_\Gamma^B(0,0,P_z,a)$$

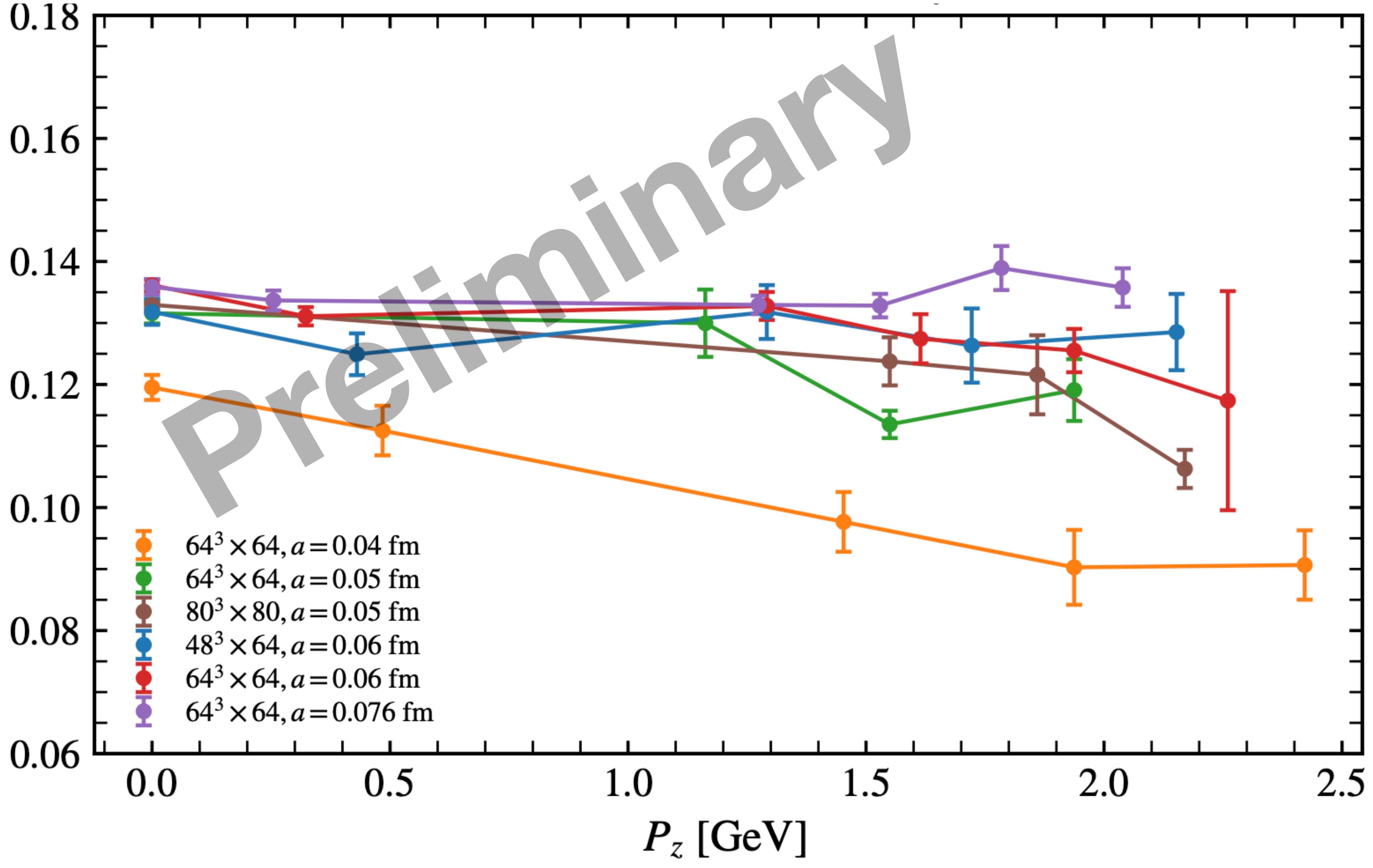

Bare decay constant $\tilde{\phi}^B(a) = f_\pi / Z_A(a)$

- broadly close to physical $f_\pi \sim 0.13$ GeV due to renormalization factor $Z_A(a) \sim 1$
- finite-volume effect visible only for smallest lattice
- decay constant of excited states are largely different: ground state under control

Quasi-TMDWF matrix elements: ratio renormalization

$$\tilde{\Phi}^{R}(b_\perp, b_z, P_z) = \frac{\tilde{\phi}^{B}_{\Gamma}(b_\perp, b_z, P_z, a)}{\tilde{\phi}^{B}_{\Gamma}(b_\perp, 0, 0, a)} \frac{\tilde{\phi}^{B}_{\Gamma}(0,0,0,a)}{\tilde{\phi}^{B}_{\Gamma}(0,0,P_z, a)}$$

Cancel the common renormalization factor $Z_q^{\mathrm{CG}}(a)$

Remove the shared systematics: FV, a^2,...

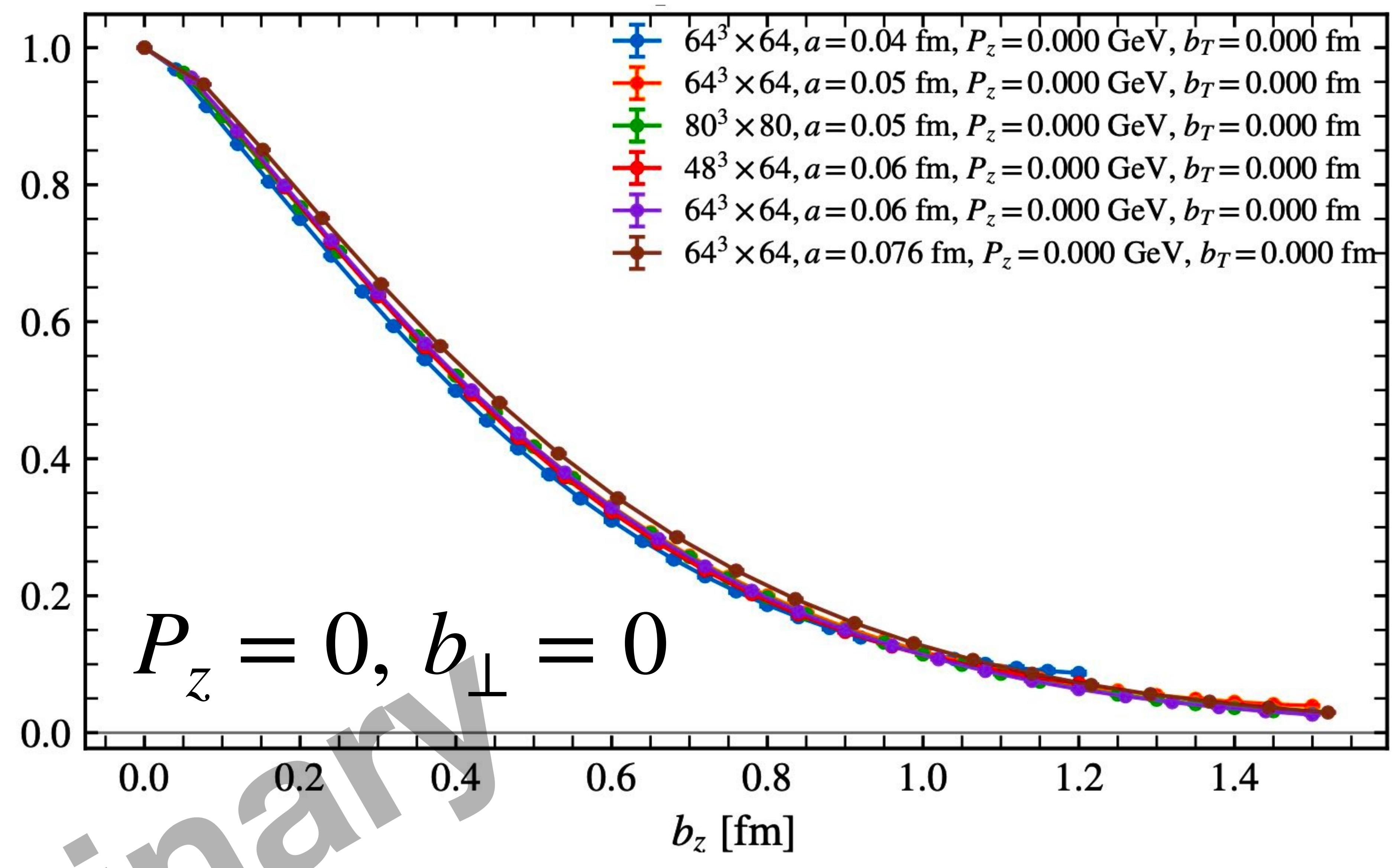

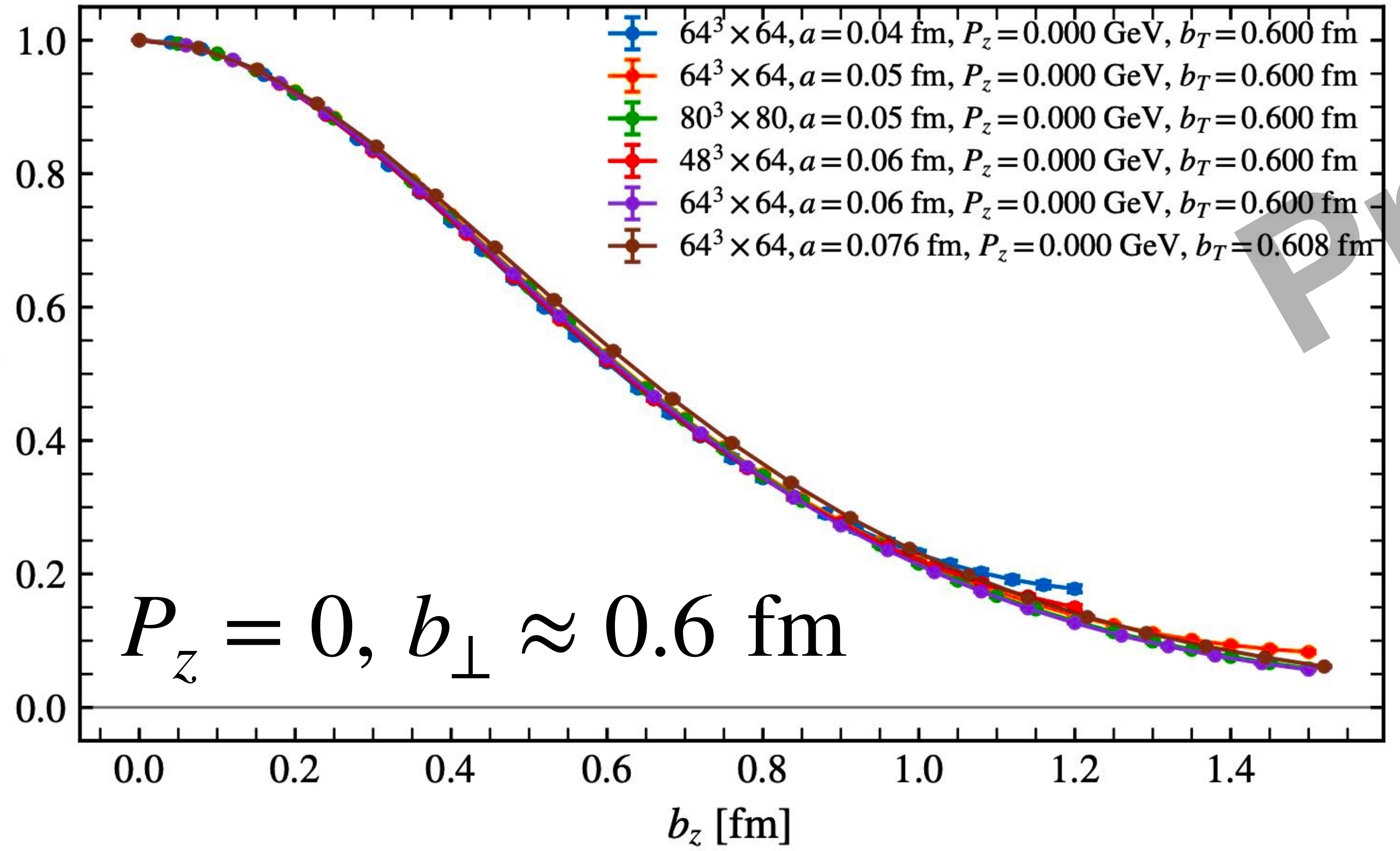

Preliminary

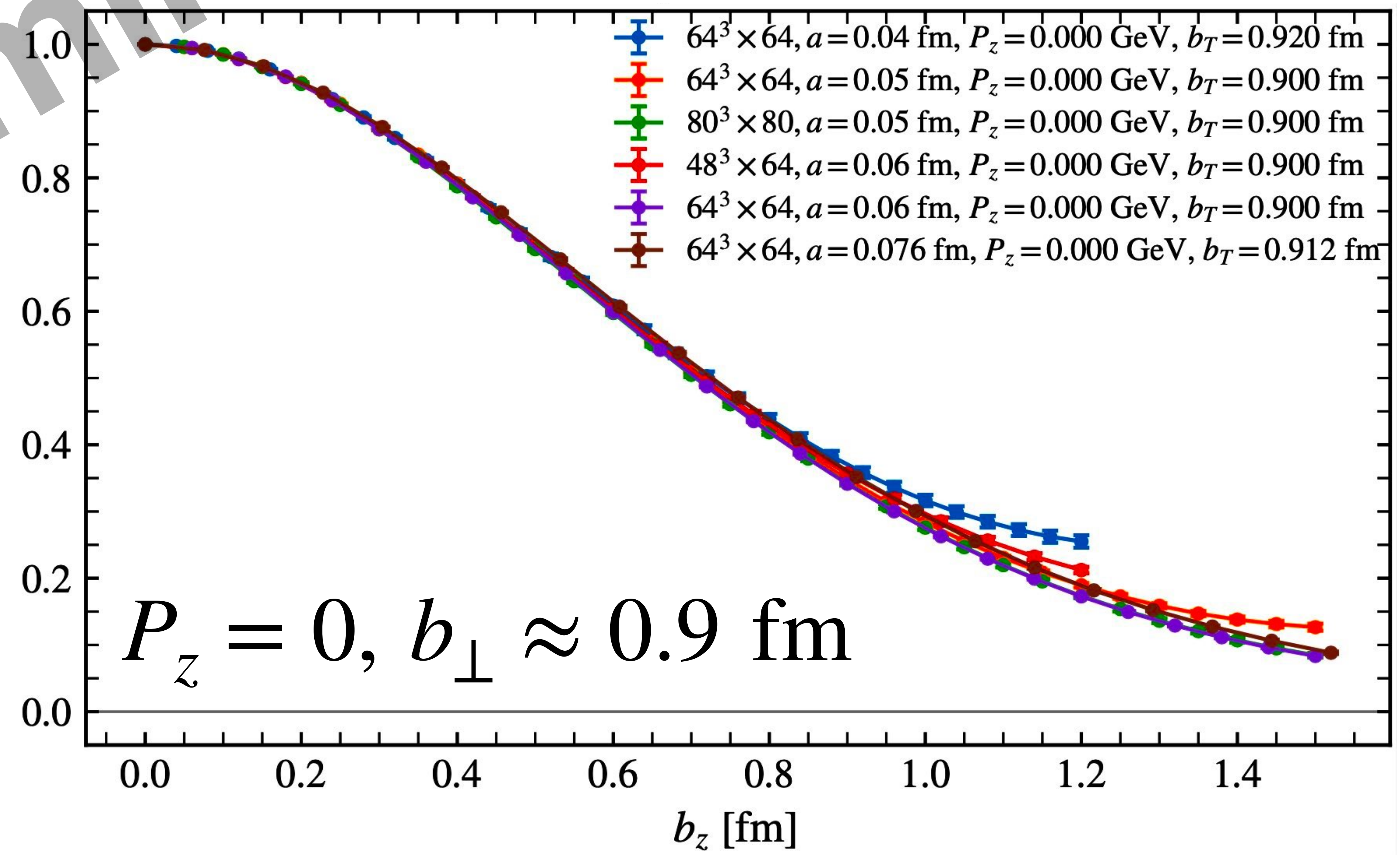

Quasi-TMDWF matrix elements: zero momentum

- **Mild discretization effect** observed: controllable continuum limit.
- **Finite-volume effect** mainly visible at **large** $b_\perp$ **and** b_z for low P_z case.

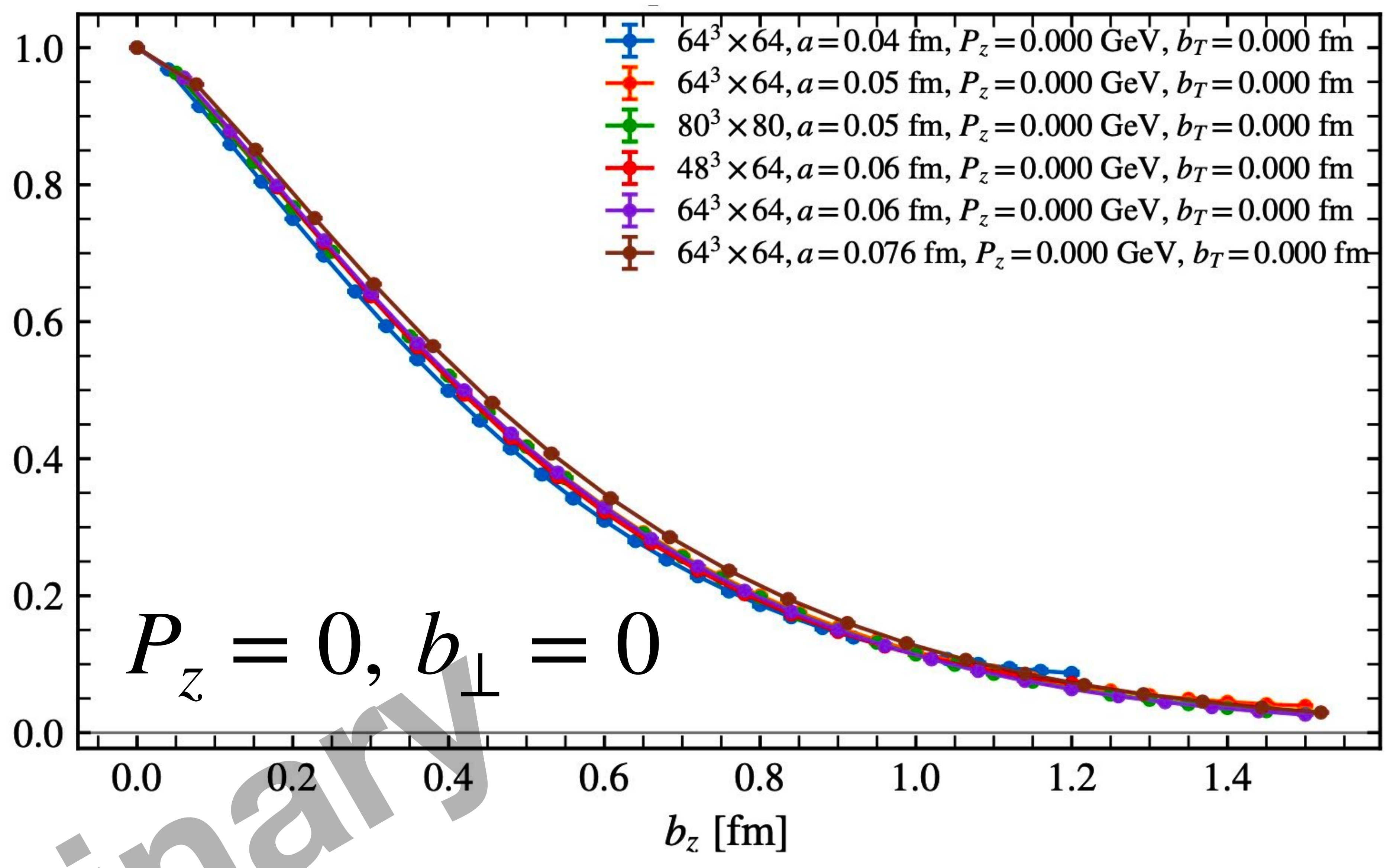

Preliminary

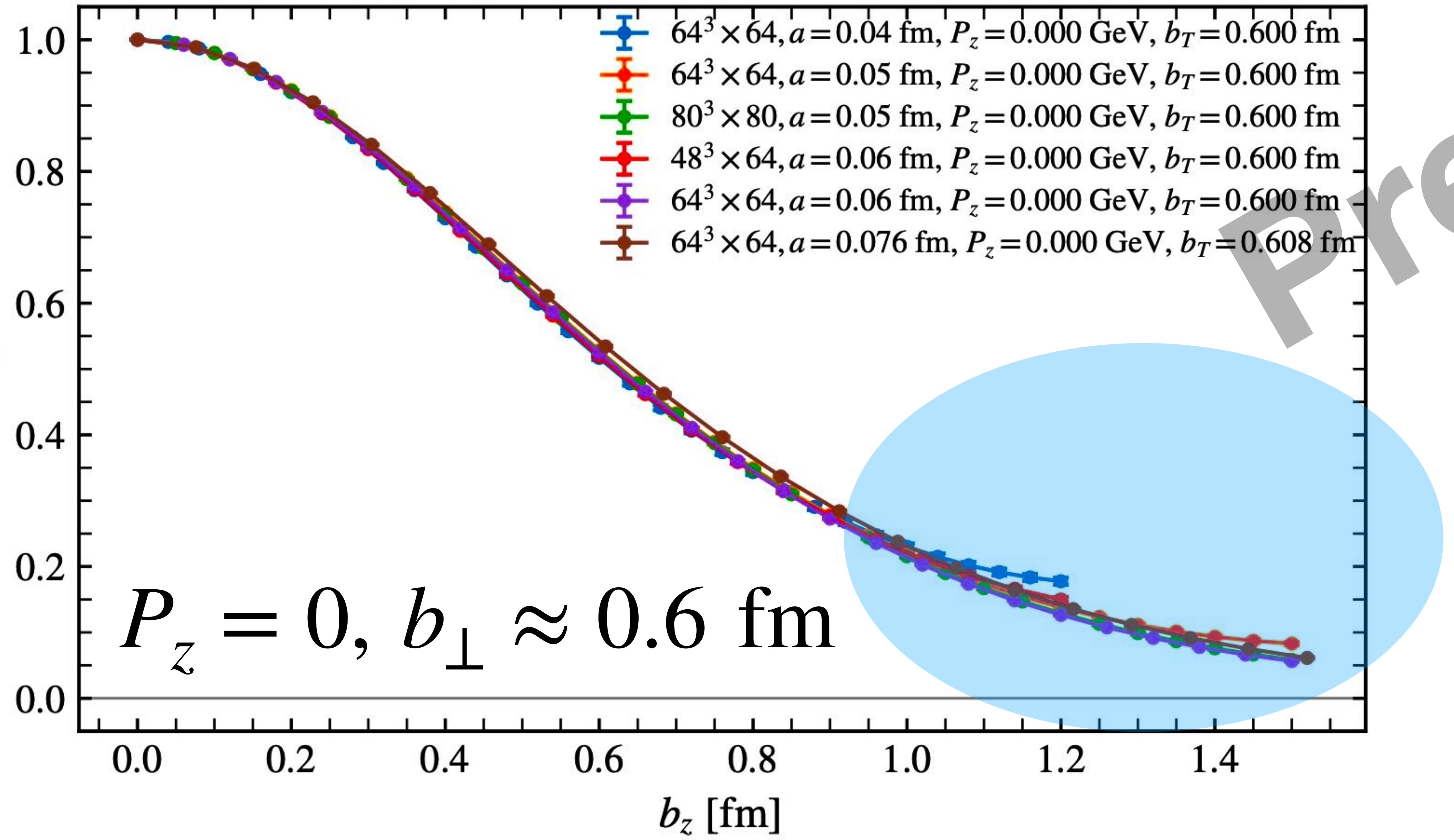

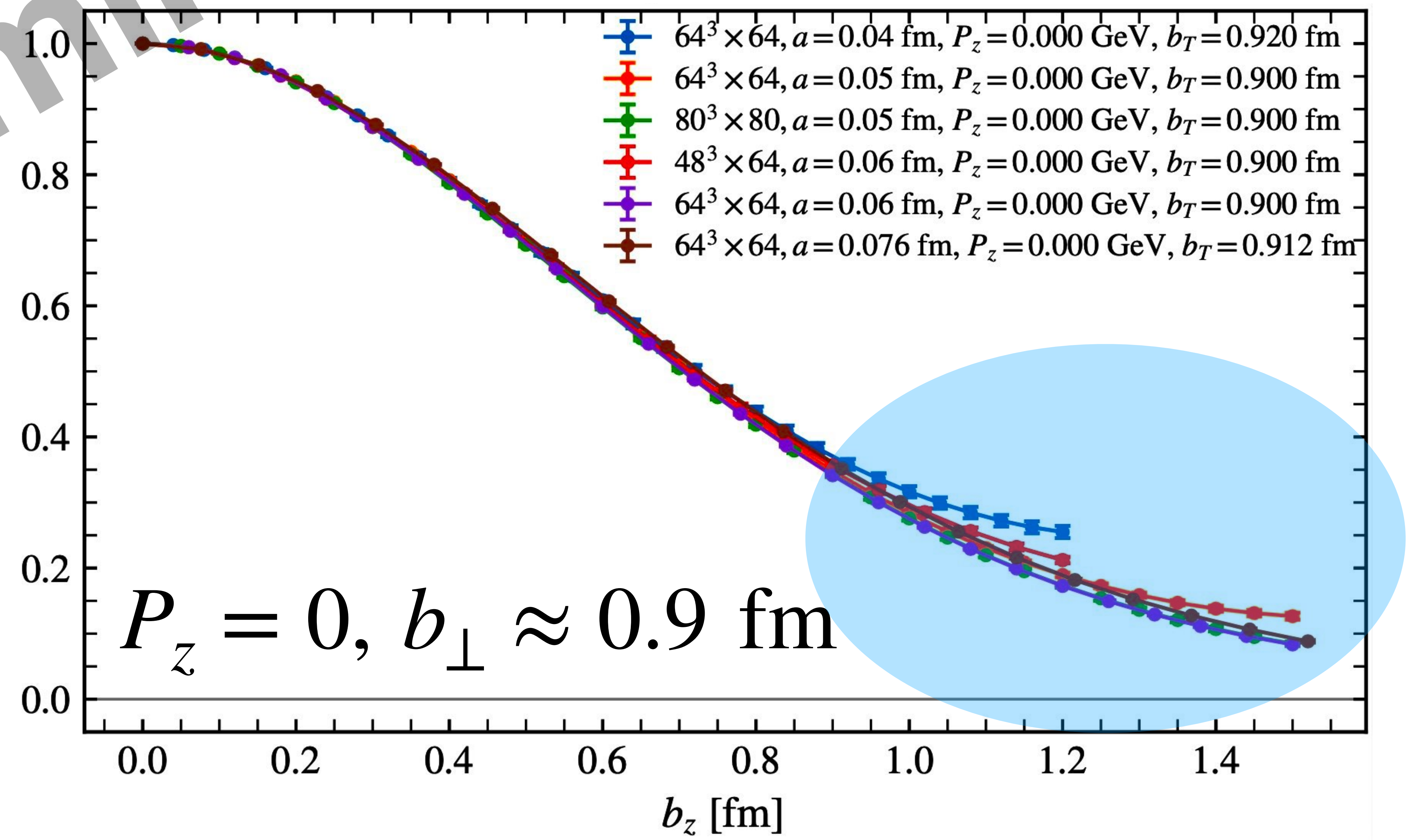

Quasi-TMDWF matrix elements: nonzero momentum

$P_z \approx 1.3$ GeV, $b_\perp \approx 0.6$ fm

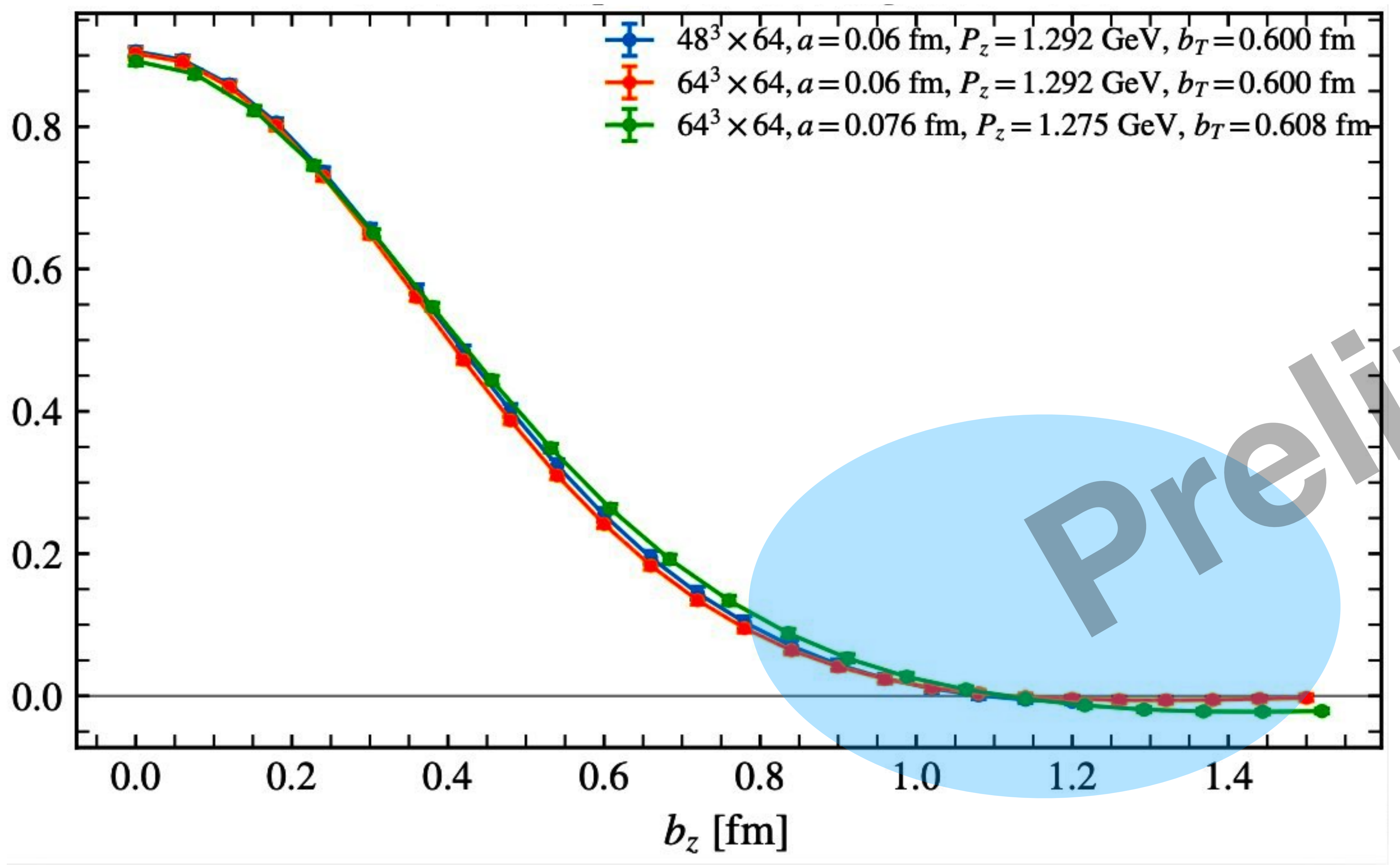

$P_z \approx 1.9$ GeV, $b_\perp \approx 0.9$ fm

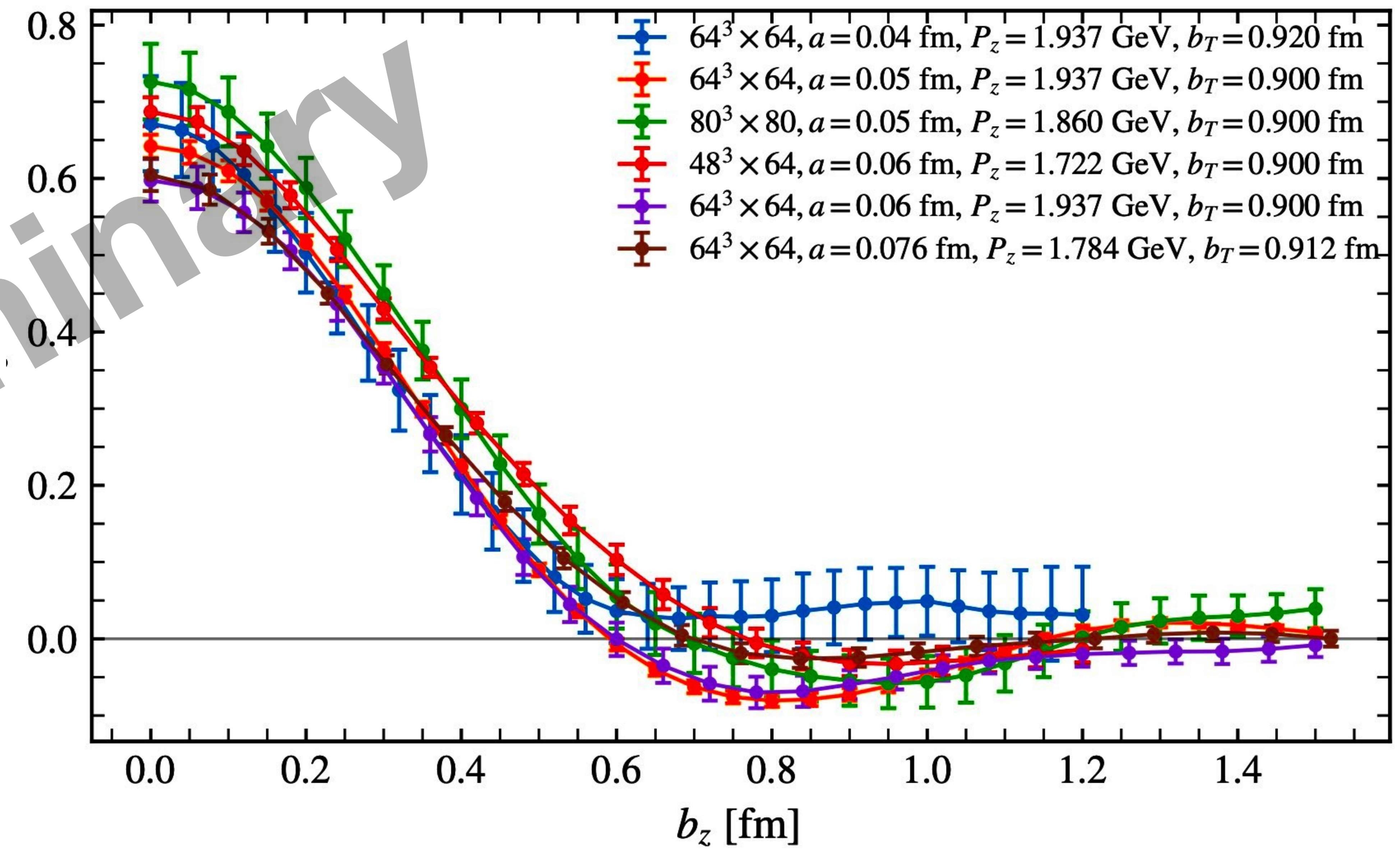

- **Finite-volume effect no longer critical** at large P_z.
- Mild ensemble dependence compared to statistical uncertainties.

Fourier-transformed quasi-TMDWFs $\tilde{\Phi}^R(x, b_\perp, P_z)$

$$\tilde{\Phi}^R(x, b_\perp, P_z) = \frac{P_z a}{\pi} \sum_{b_z=0}^{b_z^{\max}} e^{i(x-\frac{1}{2})P_z b_z} \tilde{\Phi}^R(b_\perp, b_z, P_z)$$

$64^3 \times 64,\ a = 0.05\ \text{fm};\ b_\perp \approx 1\ \text{fm}$

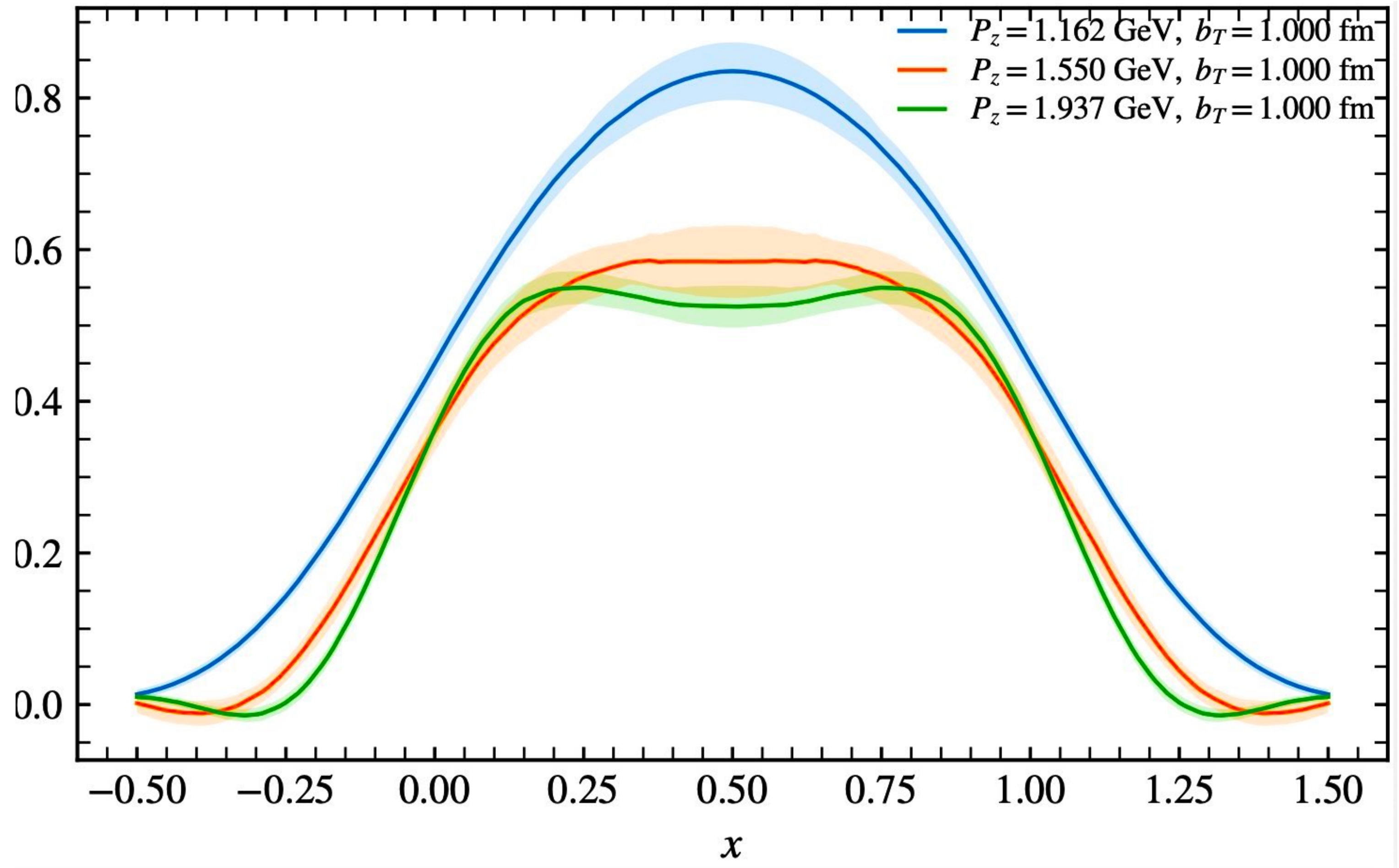

$64^3 \times 64,\ a = 0.06\ \text{fm};\ b_\perp \approx 1\ \text{fm}$

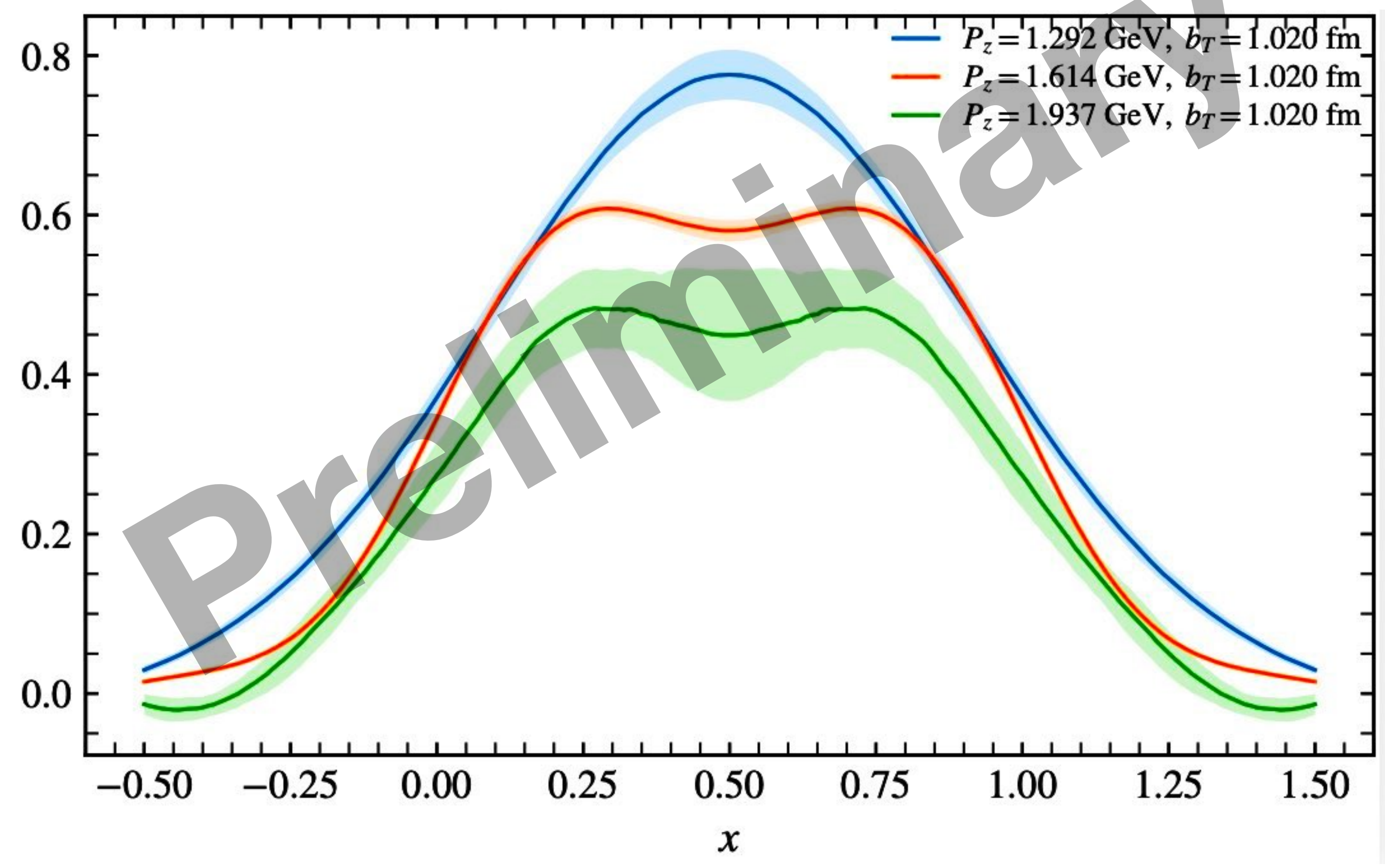

$64^3 \times 64,\ a = 0.076\ \text{fm};\ b_\perp \approx 1\ \text{fm}$

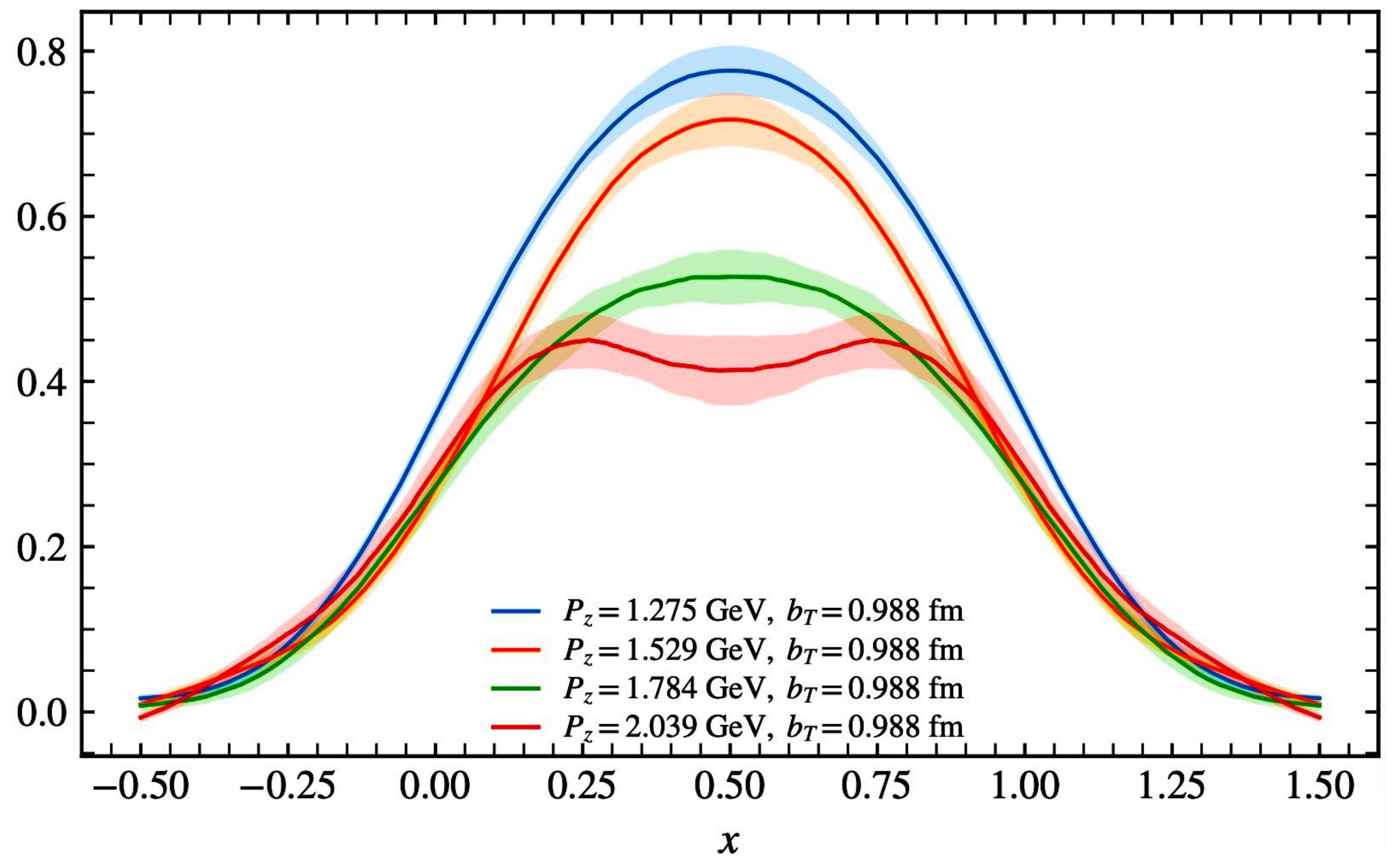

- **Reasonable signal persists** up to $b_\perp \approx 1\ \text{fm}$ and $P_z \approx 2\ \text{GeV}$.
- The P_z dependence is the input for the CS-kernel extraction.

Joint-analysis for CS kernel: fit strategy

CS kernel

perturbative correction

$$\tilde{\Phi}^R(x, b_\perp, P_z) = \tilde{\Phi}^R_{\text{ref}}(x, b_\perp, P_{\text{ref}}) \exp\left[\ln\left(\frac{P_z}{P_{\text{ref}}}\right)\left(\gamma^{\overline{\text{MS}}}(b_\perp, \mu) C_{\text{corr}} - \delta\gamma^{\overline{\text{MS}}}(x, \mu, P_{\text{ref}}, P_z)\right)\right]$$

Lattice and power correction

$\{x, b_\perp, P_z\}$-dependent quasi-TMDWF

↓

Joint-fit across ensembles

↓

Common physical CS kernels $\gamma^{\overline{\text{MS}}}(b_\perp, \mu)$

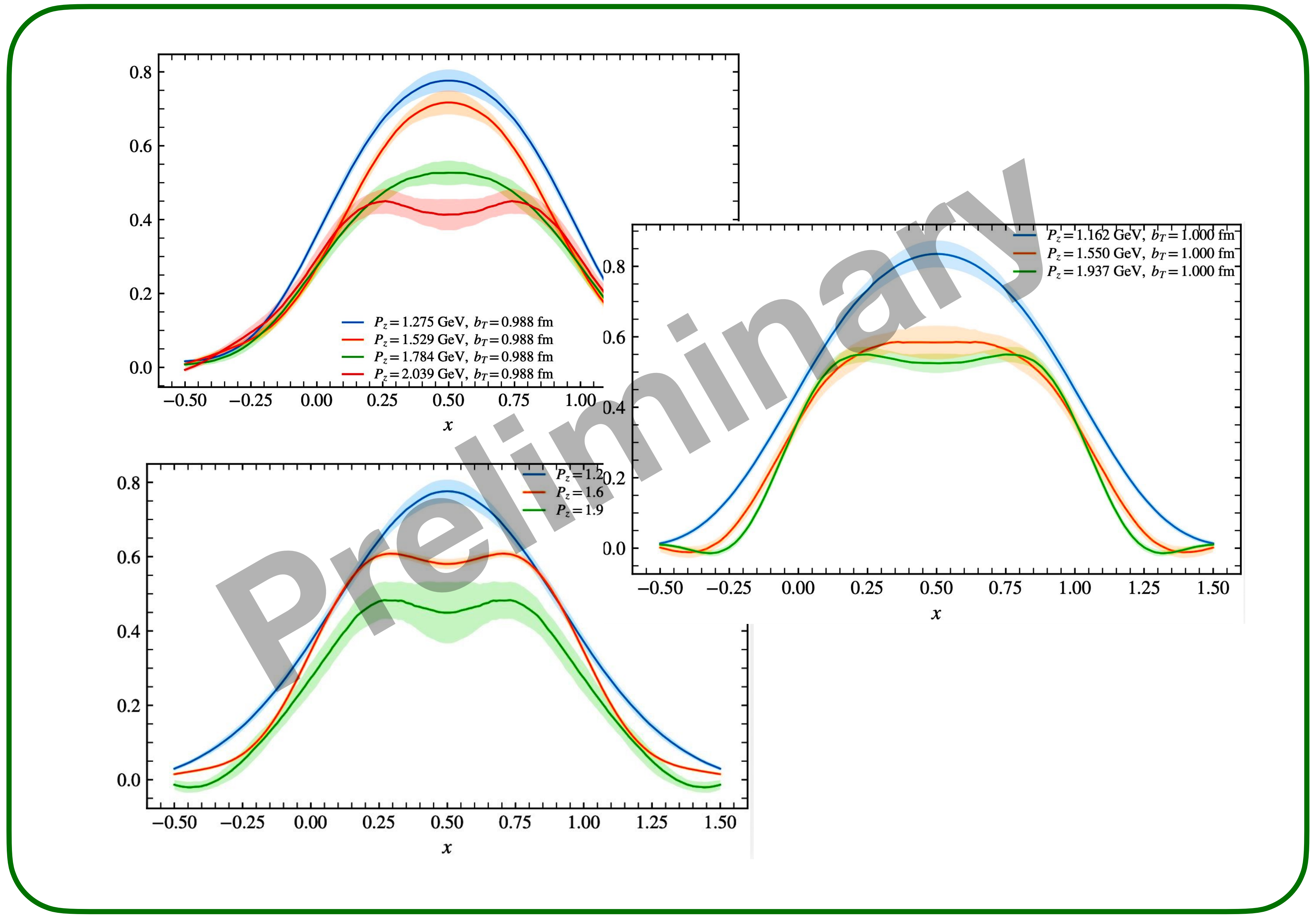

Joint-analysis for CS kernel: systematic corrections

CS kernel — perturbative correction

$$\tilde{\Phi}^R(x, b_\perp, P_z) = \tilde{\Phi}^R_{\text{ref}}(x, b_\perp, P_{\text{ref}})\exp\left[\ln\left(\frac{P_z}{P_{\text{ref}}}\right)\left(\gamma^{\overline{\text{MS}}}(b_\perp, \mu)C_{\text{corr}} - \delta\gamma^{\overline{\text{MS}}}(x, \mu, P_{\text{ref}}, P_z)\right)\right]$$

Lattice and power correction

$\{x, b_\perp, P_z\}$-dependent quasi-TMDWF

↓

Joint-fit across ensembles

↓

Common physical CS kernels $\gamma^{\overline{\text{MS}}}(b_\perp, \mu)$

$$C_{\text{corr}} = 1 + \left(\frac{a}{a_0}\right)^2\left[\alpha_0 + \alpha_1\left(\frac{b_0}{b_\perp}\right)^2\right]$$

Continuum extrapolation

$$+\frac{e^{-M_\pi L}}{\sqrt{M_\pi L}}\left[\beta_0 + \beta_1 e^{M_\pi b_\perp}\right]$$

F.V. corrections

$$+\left(\frac{p_0}{P_z}\right)^2\left(\frac{1}{x^2} + \frac{1}{(1-x)^2}\right)\left[\kappa_0 + \kappa_1\left(\frac{b_0}{b_\perp}\right)^2\right]$$

Finite-momentum power corrections

Preliminary

Joint-analysis for CS kernel: spline reconstruction

CS kernel　　　　perturbative correction

$$\tilde{\Phi}^R(x, b_\perp, P_z) = \tilde{\Phi}^R_{\text{ref}}(x, b_\perp, P_{\text{ref}}) \exp\left[\ln\left(\frac{P_z}{P_{\text{ref}}}\right)\left(\gamma^{\overline{\text{MS}}}(b_\perp, \mu) C_{\text{corr}} - \delta\gamma^{\overline{\text{MS}}}(x, \mu, P_{\text{ref}}, P_z)\right)\right]$$

Lattice and power correction

$\{x, b_\perp, P_z\}$-dependent quasi-TMDWF

↓

Joint-fit across ensembles

↓

Common physical CS kernels $\gamma^{\overline{\text{MS}}}(b_\perp, \mu)$

Spline parameterization

$$\gamma^{\overline{\text{MS}}}(b_\perp, \mu) = \sum_{k=1}^{K} \gamma_k I_k(b_\perp)$$

- Interpolating non-common $b_\perp$ grids across ensembles with minimal model dependence.

Joint-analysis for CS kernel

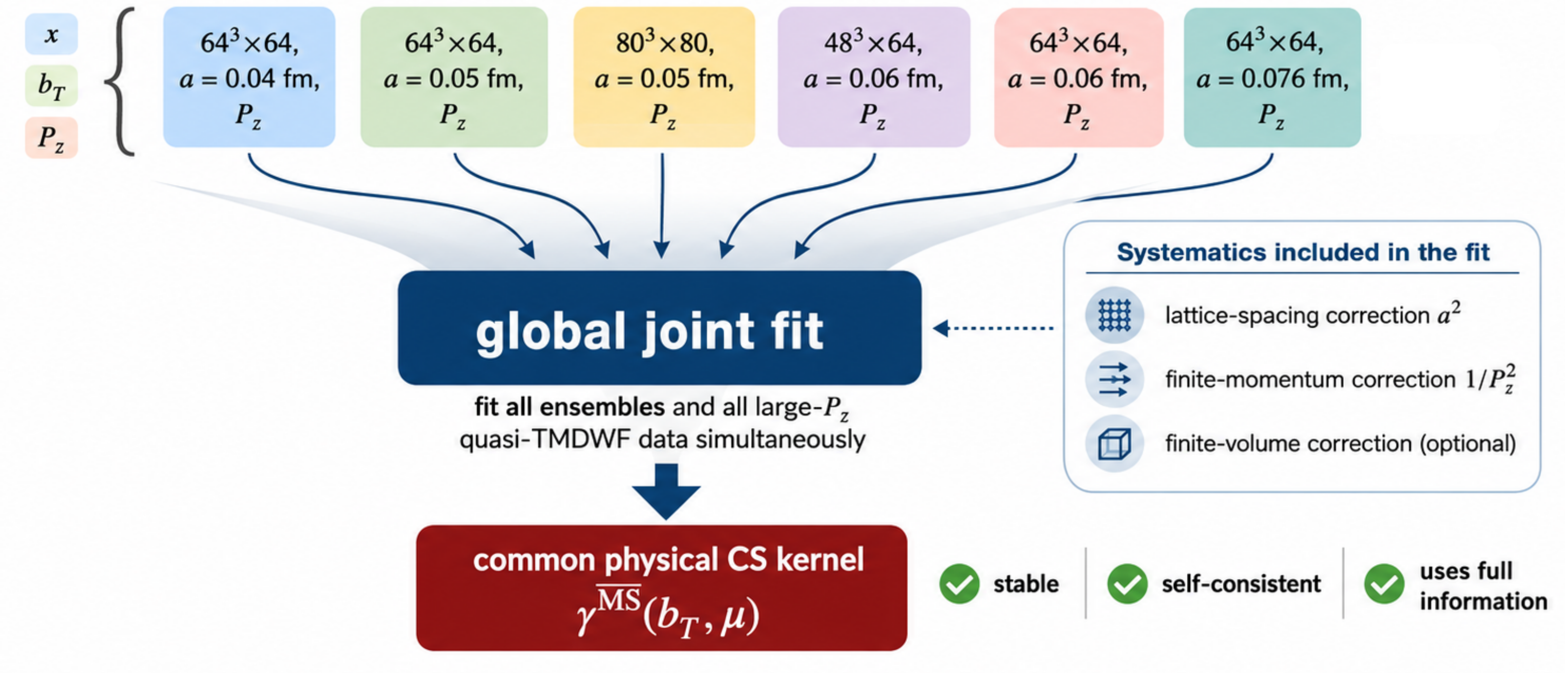

Instead of (*not done here*) → Each ensemble → Each Pz pair → Extract CS kernel first → Combine later

Joint-fit quality: Pz-dependence of quasi-TMDWF

Joint fit results for $64^3 \times 64,\ a = 0.076$ fm: $\tilde{\Phi}^R(x = 0.4, b_\perp, P_z; a)$

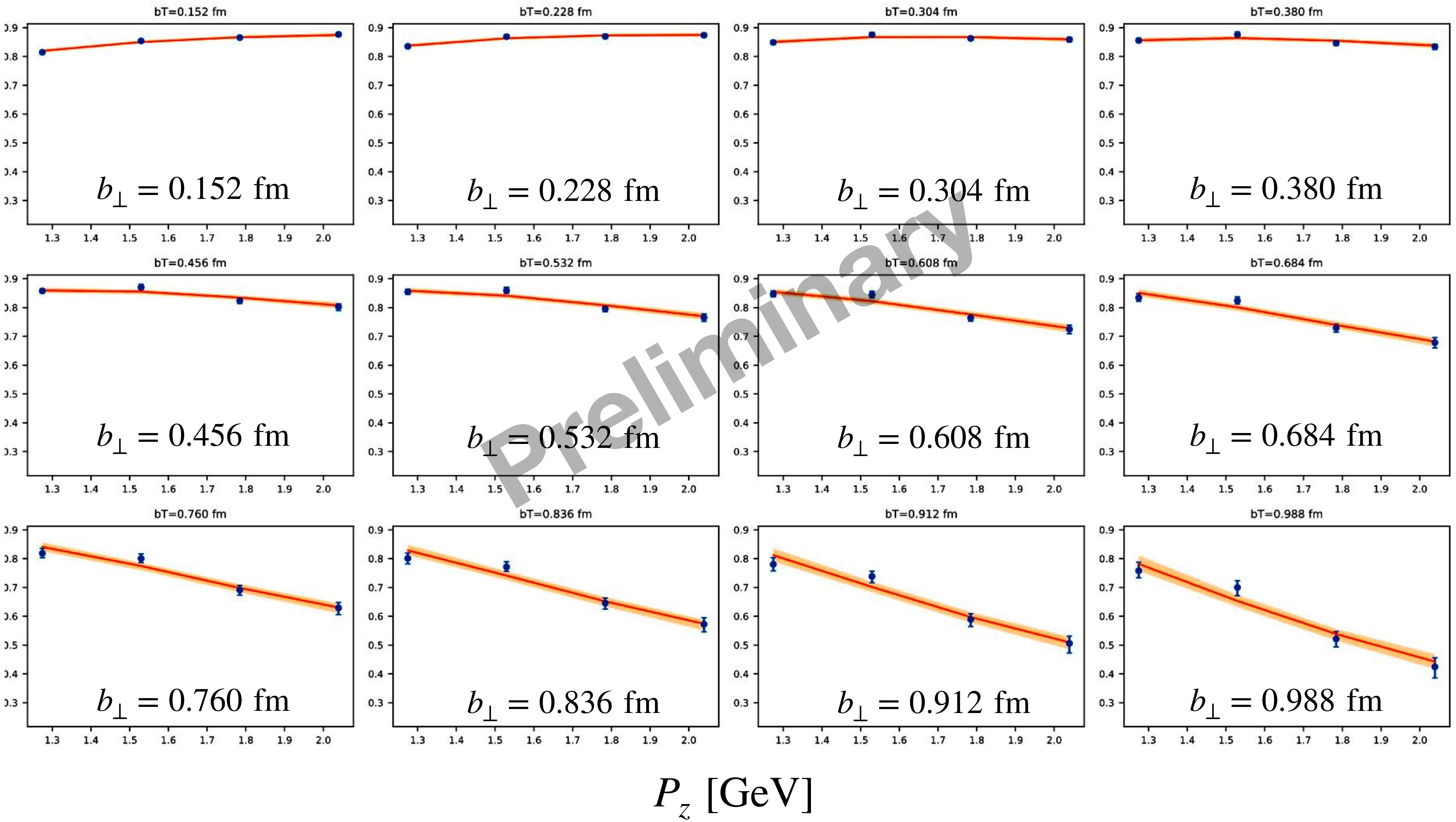

Joint-fit quality: Pz-dependence of quasi-TMDWF

Joint fit results for $64^3 \times 64,\ a = 0.076$ fm: $\tilde{\Phi}^R(x = 0.4, b_\perp, P_z; a)$

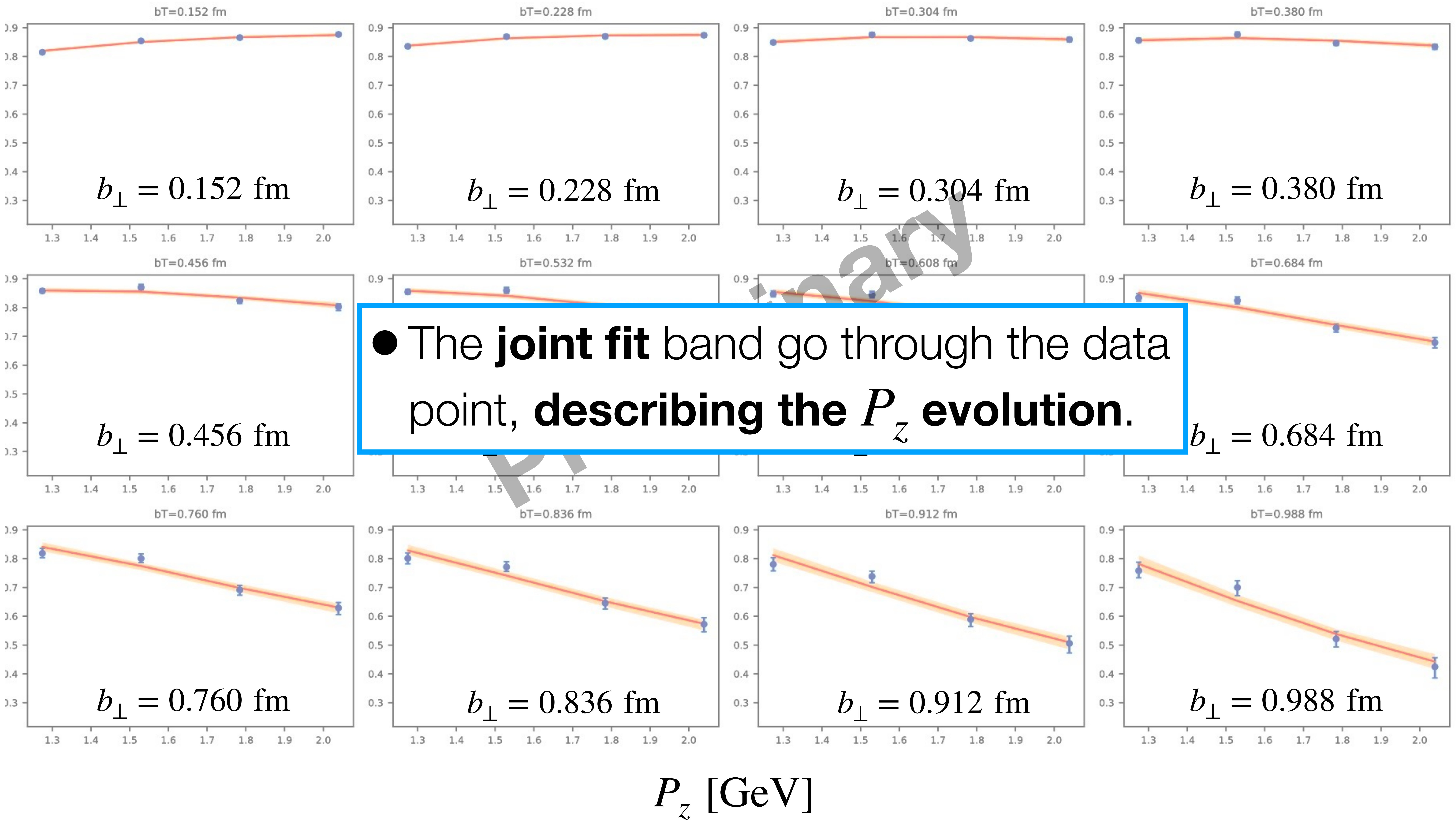

- The **joint fit** band go through the data point, **describing the P_z evolution**.

Joint-fit quality: Pz-dependence of quasi-TMDWF

Joint fit results for $64^3 \times 64,\ a = 0.076\ \text{fm}$**:** $\tilde{\Phi}^R(x = 0.4, b_\perp, P_z; a)$

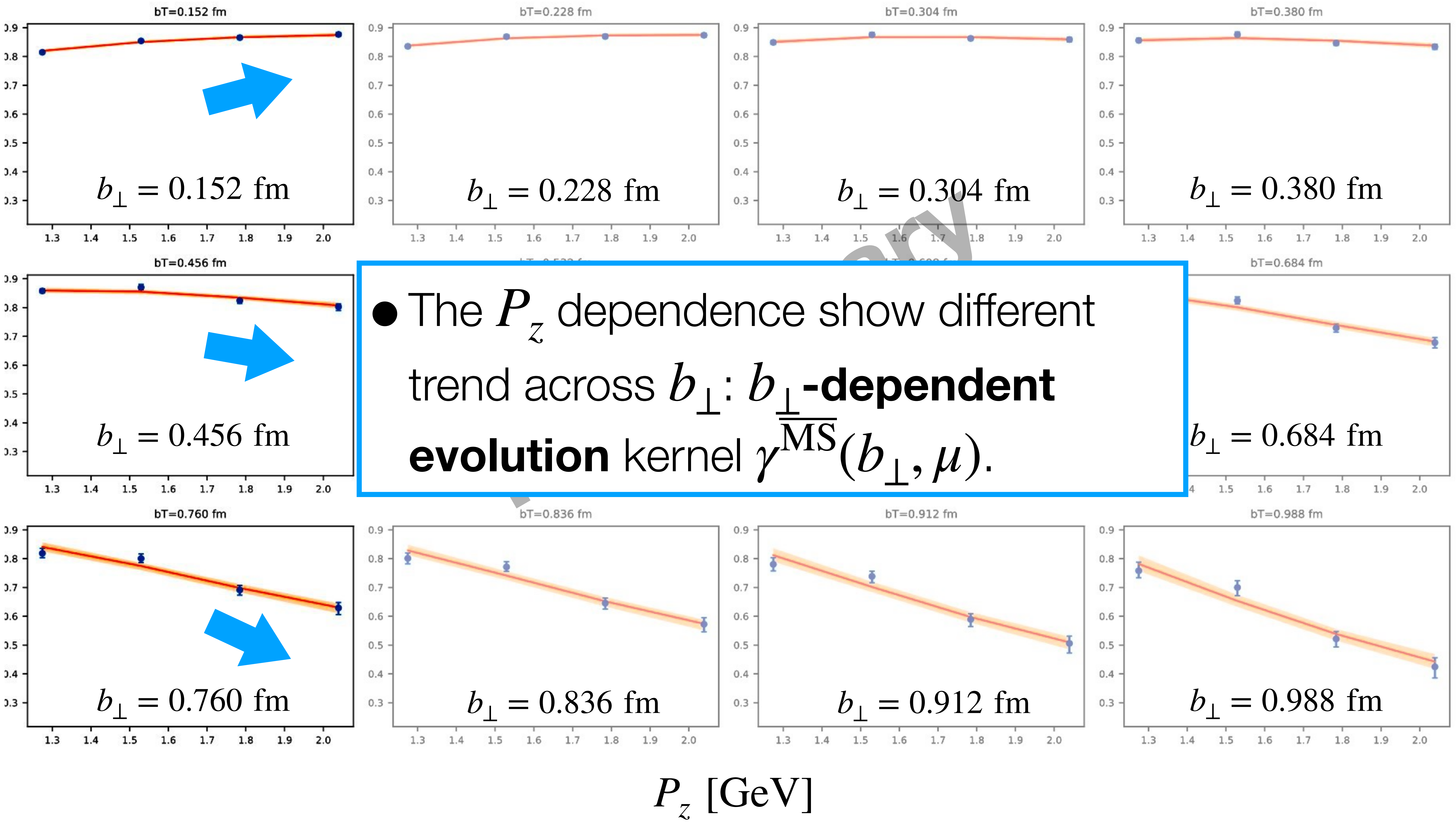

- The P_z dependence show different trend across $b_\perp$: $b_\perp$**-dependent evolution** kernel $\gamma^{\overline{\text{MS}}}(b_\perp, \mu)$.

Joint-fit quality: Pz-dependence of quasi-TMDWF

Joint fit results for other ensembles: $\tilde{\Phi}^R(x = 0.4, b_\perp, P_z; a)$

$64^3 \times 64,\ a = 0.04$ fm | $64^3 \times 64,\ a = 0.05$ fm | $80^3 \times 80,\ a = 0.05$ fm | $48^3 \times 64,\ a = 0.06$ fm | $64^3 \times 64,\ a = 0.06$ fm

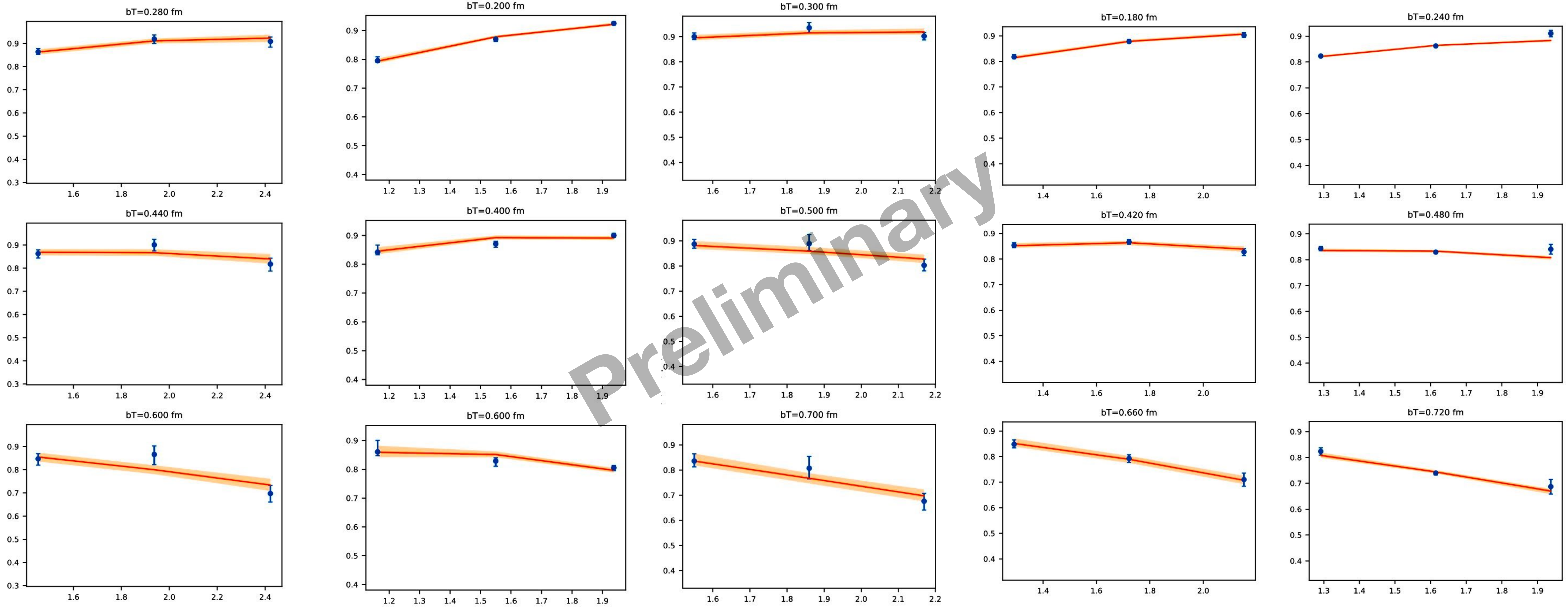

P_z [GeV]

Impact of lattice-spacing and finite-Pz corrections

Ensemble trend and joint-fit extrapolation

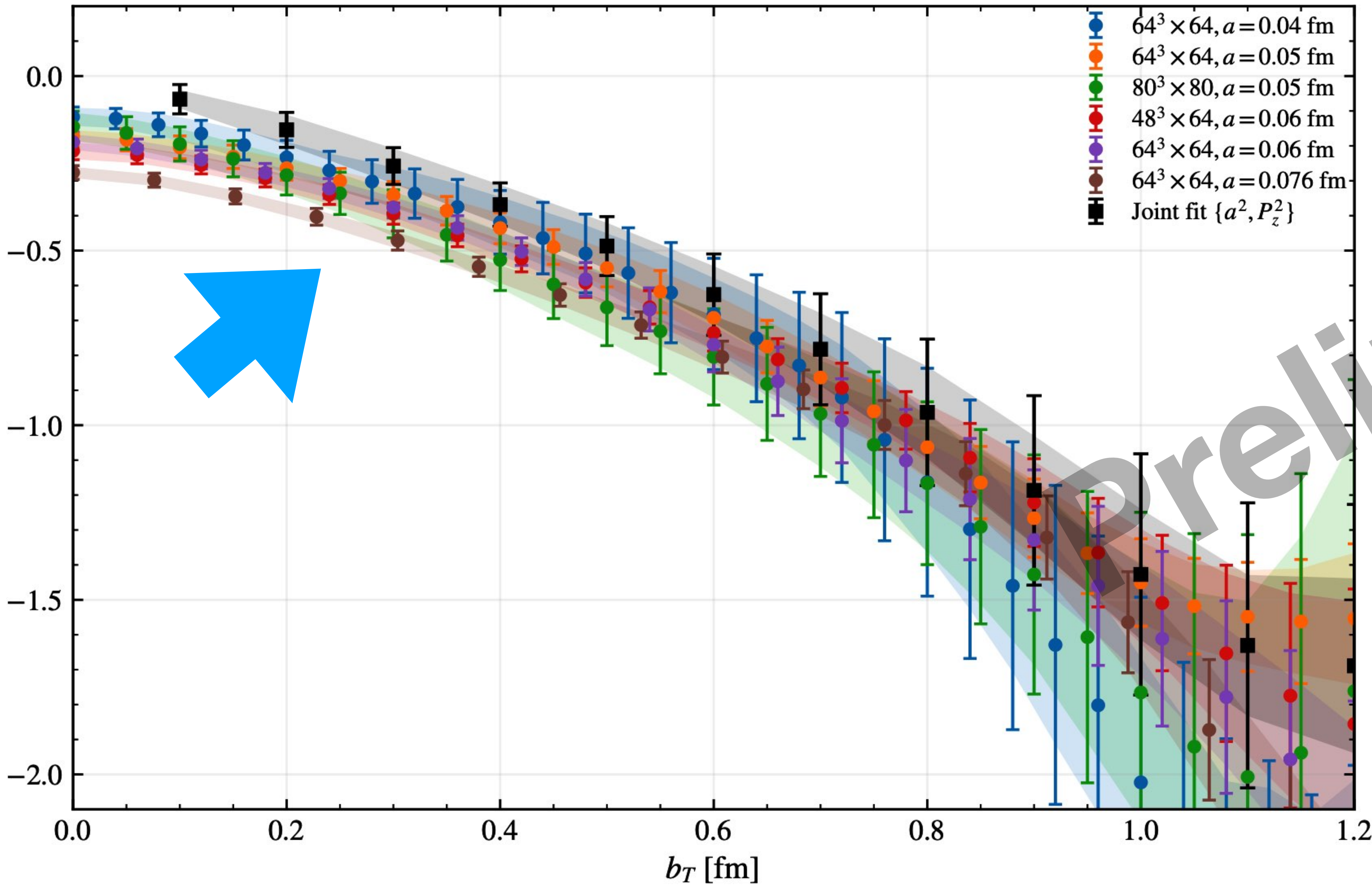

Comparison between different corrections

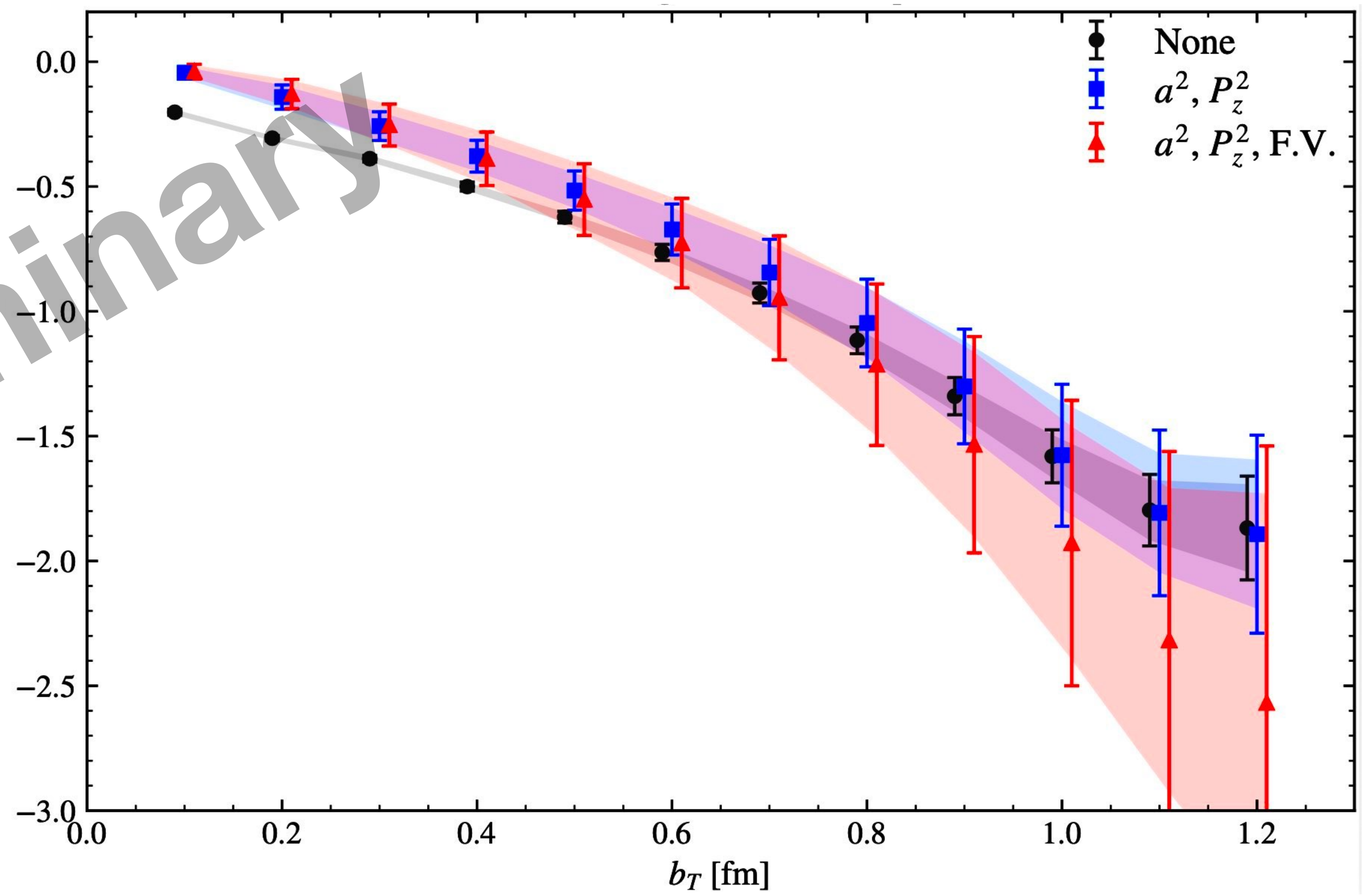

- At small $b_\perp$, a visible a^2 dependence is present and the **joint fit follows the ensemble trend**.
- The dominant improvement comes from **lattice-spacing and finite-P_z corrections** while finite-volume effects are subleading.

Physical-continuum CS kernel

x-dependence of the fitted CS kernel

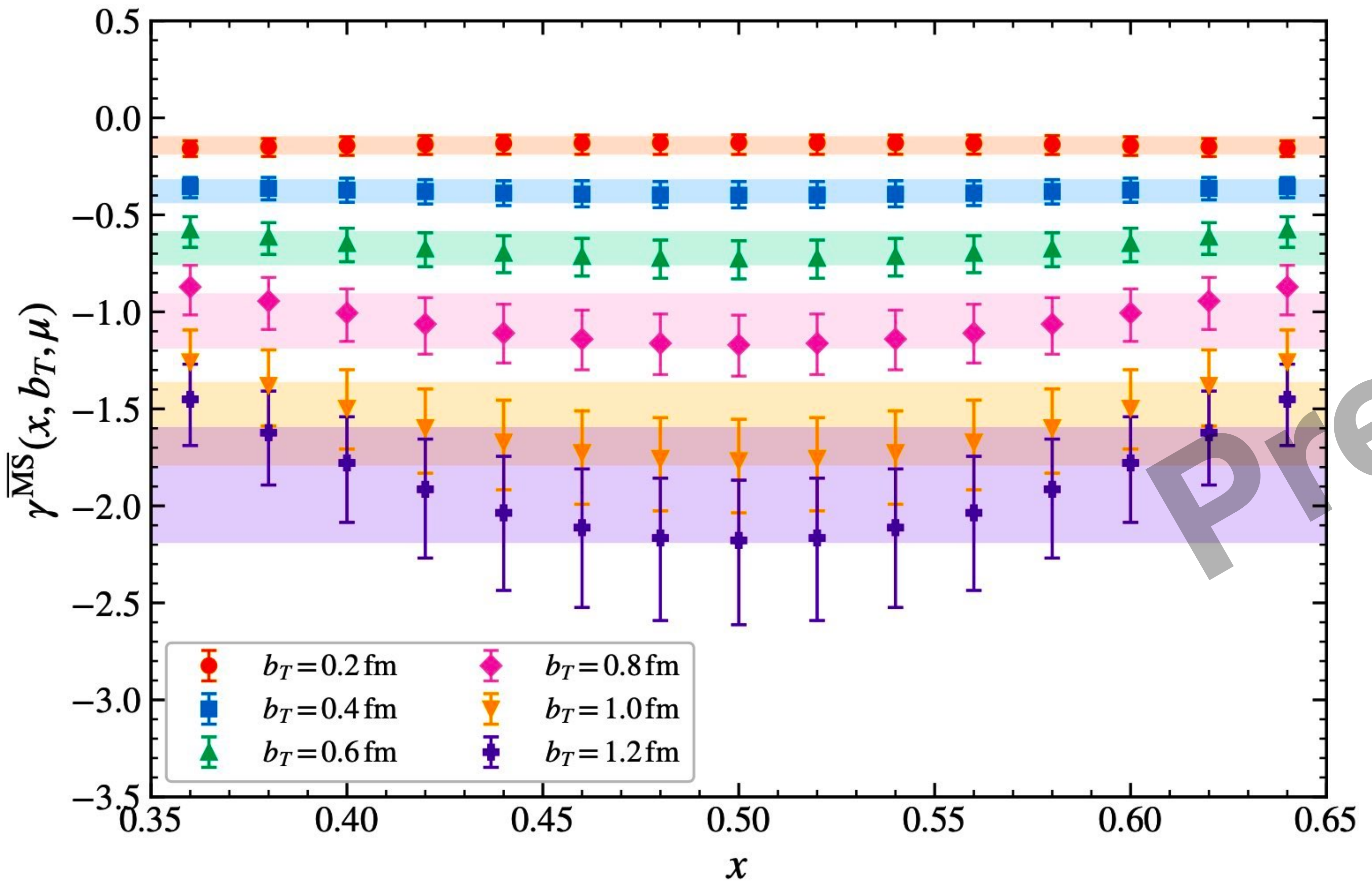

Comparison with various pheno. and Lat.

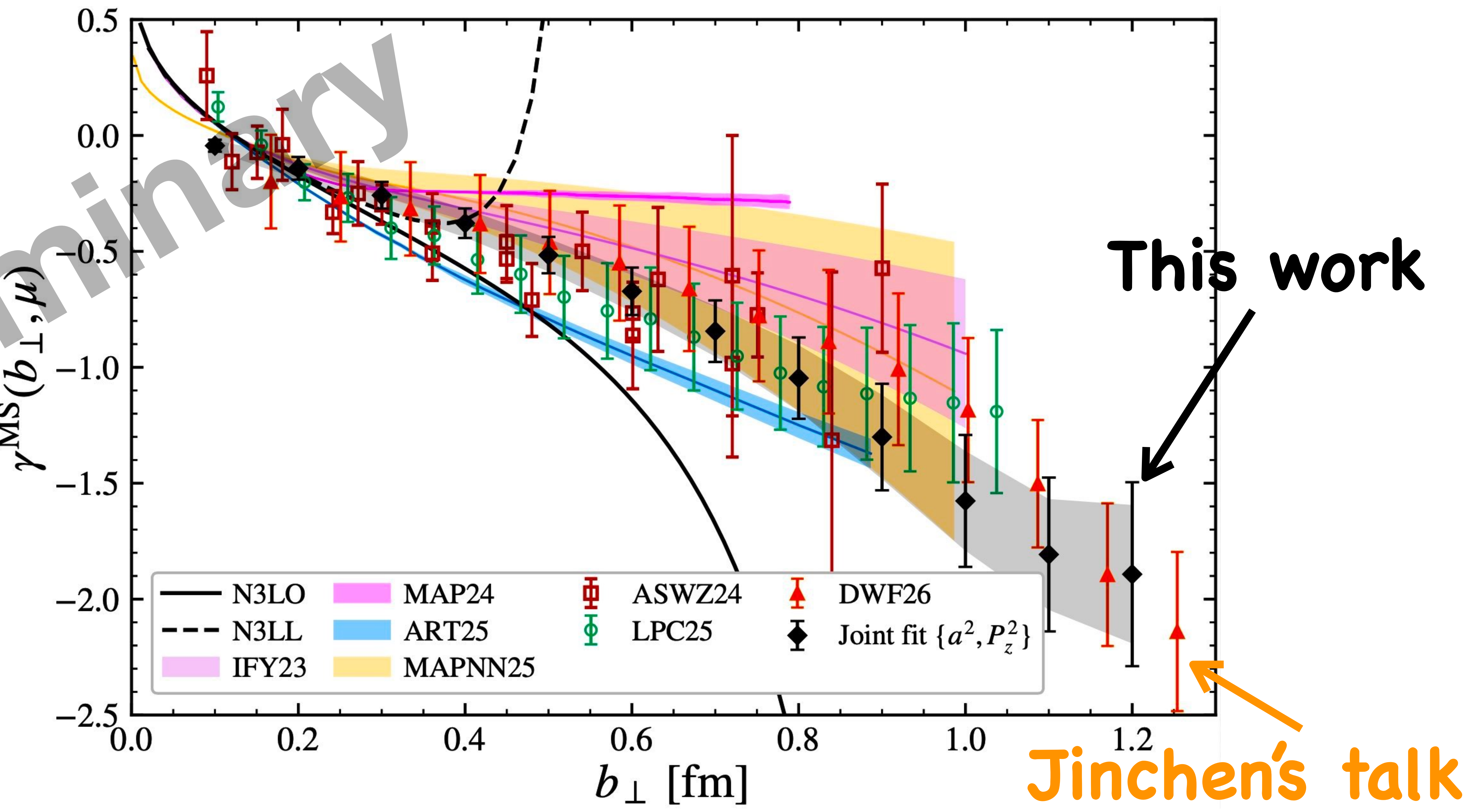

- The fitted CS kernel is approximately x**-independent** over the fit window, indicating controlled finite-Pz effects at current precision.
- **Reach** $b_\perp \approx 1.2$ fm **with reasonable signal** and **broadly consistent** with pQCD, phenomenological parametrization, lattice calculation at shorter $b_\perp$.

Summary & outlook

- Coulomb-gauge quasi-TMD correlators offer an efficient lattice approach to TMD observables within LaMET.
- The method has shown its effectiveness in the extraction of CS-kernel and nucleon-TMDPDF calculations at physical quark masses.
- We are now moving toward a physical-mass continuum determination of the CS kernel.
- Outlook: extend this framework to broad TMD studies, with improved control of matching, power corrections, and lattice systematics.

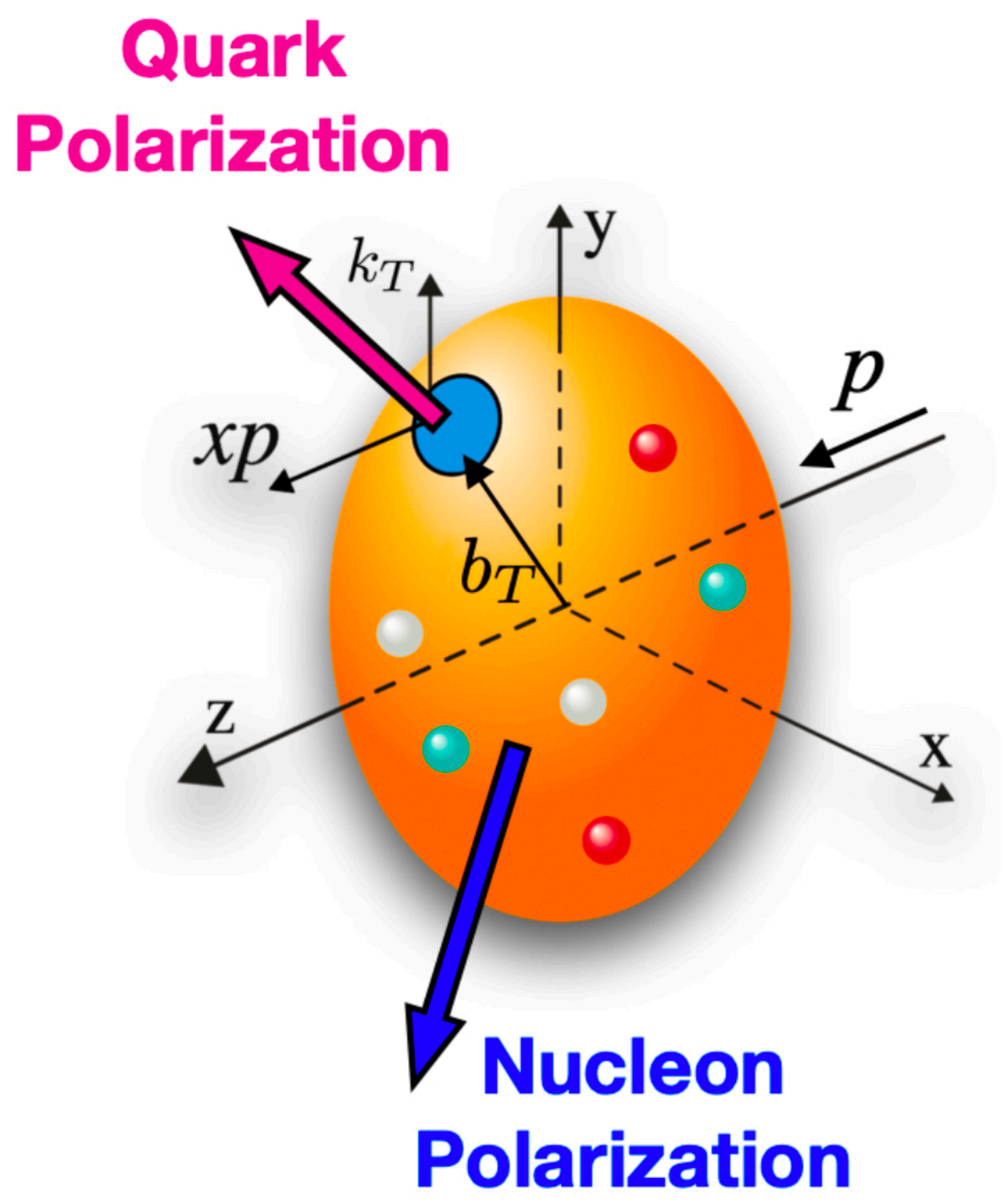

Thanks for your attention!